

Host Immunity Determines Outcome of Eukaryotic Initiation Factor-4A Inhibition in Breast Cancer

by

Igor Zlobine

A thesis submitted to McGill University in partial fulfillment of the requirements of the degree
of

Master of Science

in

Biochemistry

Department of Biochemistry
McGill University, Montreal

Submitted: June 2018

© Igor Zlobine, 2018

ABSTRACT

Breast cancer will affect one in eight Canadian women during their lifetime. Furthermore, amongst all breast cancer subtypes, triple-negative breast cancer (TNBC) is the deadliest due to a lack of targeted therapies. One potential way to address this problem is by targeting translation, as abnormal translation of cellular mRNAs is a common feature in many types of cancers, including breast. The RNA helicase eukaryotic translation initiation factor 4A (eIF4A), and the mRNA cap-binding protein eIF4E, are both components of the eIF4F complex. eIF4F is particularly efficient at targeting mRNAs with short half-lives such as Cyclin D1, anti-apoptotic proteins including Bcl-2, and other factors important in tumorigenesis such as TGF- β , and VEGF. eIF4A specifically targets mRNA transcripts with complex G/C-rich 5' UTR sequences such as those capable of forming RNA G-quadruplex structures, and it helps to unwind these structured mRNAs to facilitate ribosome scanning. Targeting various components of the eIF4F complex has emerged as a potential therapeutic target in cancer, given that translation initiation is a critical nexus since it is the rate-limiting step in protein synthesis. In addition, targeting upstream eIF4F signalling components such as mTOR, often leads to therapeutic resistance, and compensatory mechanisms. mTOR inhibitors have shown utility in ER+ patients, but have so far been unsuccessful in TNBC, which may be due to inefficient targeting of translation. eIF4E has been extensively studied as a potential therapeutic target in cancer, and although modulating eIF4E provides promising results in pre-clinical assessment, a recent phase I/II clinical trial using antisense oligonucleotides against eIF4E did not produce particularly favourable results. Thus, the purpose here was to explore the idea that targeting eIF4A might be preferable to targeting eIF4E or mTOR, since a recent publication outlined distinct eIF4A and eIF4E-dependent mRNAs are preferentially targeted by these initiation factors, and eIF4A inhibitors are more

potent than those targeting mTOR. Furthermore, tissue microarray analysis from over 3000 breast tumors demonstrated that eIF4A is an independent predictor of poor outcome in ER- patients. The small molecule eIF4A inhibitor silvestrol has shown impressive potential in various cancers, including breast. CR-1-31-B (which is used here) is the synthetic derivative of silvestrol, which has a simplified chemical structure, allowing for more efficient synthesis. The murine TNBC cell line, 4T1 was used as a model, as it recapitulates all stages of human breast cancer, from primary tumour development, up until metastasis. This idea was to test it in both immune-competent, and immune-compromised mice. This thesis thus expands on our current knowledge and understanding of how translation inhibitors influence TNBC tumour growth, and how they interact with the tumour microenvironment.

Résumé

Une Canadienne sur huit sera touchée par le cancer du sein au cours de sa vie. De tous les sous-types, le cancer du sein triple-négatif est la forme la plus mortelle due à l'absence de thérapie ciblée. Une façon de s'attaquer à ce problème est de cibler la traduction d'ARNm en protéines, puisque la traduction anormale est une caractéristique commune de plusieurs cancers, dont le cancer du sein. Le facteur d'initiation de la traduction eIF4A, une hélicase à ARN, et la protéine liant la coiffe des ARNm, eIF4E, sont deux composantes du complexe eIF4F. L'activité d'eIF4F est particulièrement importante pour assurer l'expression de facteurs clés dans la tumorigénèse, tels que le facteur de croissance transformant β (TGF β), le facteur de croissance de l'endothélium vasculaire (VEGF), la cycline D1, ainsi que des protéines anti-apoptotiques de la famille Bcl2. De par son activité hélicase, eIF4A promeut spécifiquement la traduction d'ARNm dont la séquence non-traduite en 5' (5'UTR) comporte des éléments favorisant la formation de structures secondaires ou tertiaires stables, tel que des G-quadruplexes, pour permettre le balayage de l'ARNm par le ribosome. Les molécules ciblant les composantes du complexe eIF4F présentent un potentiel intéressant pour le traitement du cancer, puisque l'initiation de la traduction est l'étape limitante dans la synthèse protéique et donc un nœud critique des cellules cancéreuses. De plus, l'inhibition des facteurs de signalisation en amont d'eIF4F, telle que la kinase mTOR, mène fréquemment à la résistance au traitement causée par des mécanismes de signalisation compensatoires. Les inhibiteurs de mTOR démontrent des bienfaits chez les patientes atteintes de cancer du sein exprimant le récepteur de l'œstrogène (ER+), mais ne semblent pas efficaces dans le traitement des tumeurs triple-négatives, potentiellement due à une inhibition de la traduction inefficace. Les molécules ciblant eIF4E ont été abondamment étudiées, et sont fort efficaces dans des modèles pré-cliniques, mais ont récemment échouées en essai clinique de

phase I/II. Ainsi, l'objectif des expériences présentées ici était d'explorer une approche alternative : cibler eIF4A au lieu de mTOR ou eIF4E, puisque des recherches récentes ont démontré de tels inhibiteurs sont plus puissants que ceux ciblant mTOR et affectent l'expression d'un sous-groupe différent d'ARNm. De plus, l'analyse de plus de 3000 tumeurs mammaires de patients indique que l'expression d'eIF4A est un facteur indépendant de pronostic chez les patientes triple-négatives. L'inhibiteur d'eIF4A silvestrol démontre des effets anti-cancer impressionnant dans des cellules et modèles de souris. Son dérivé synthétique, CR-1-31-B, plus facile à produire, est utilisé au cours de la présente étude. La lignée cellulaire triple-négative 4T1, isolée d'une tumeur mammaire de souris, est utilisé comme modèle pré-clinique, puisqu'elle récapitule toutes les étapes du cancer du sein chez les humains, de la formation de la tumeur au développement de métastases. Ces cellules ont été utilisées dans des souris immuno-supprimées et des souris avec un système immunitaire intacte. Cette thèse étend donc les connaissances actuelles sur l'effet des inhibiteurs de la traduction sur la croissance des tumeurs triple-négatives, ainsi que leur effet sur le micro-environnement tumoral.

If you can't explain it simply, you don't understand it well enough.

- Albert Einstein

DEDICATION

I dedicate this thesis to my wife, Anastasia Greenberg. For so many years you have always been there for me. You've been with me each step of the way. There is no way this thesis would have been possible without you.

ACKNOWLEDGMENTS:

I would like to sincerely thank and acknowledge my supervisor, Nahum Sonenberg. It has been an amazing opportunity to work in the lab of a world-famous scientist. Your decades of scientific experience, and scientific curiosity always shine through. You have allowed for my continued growth as a scientist, and have provided invaluable mentorship.

There are numerous members of the Sonenberg lab that deserve acknowledgment, but I would like to particularly thank Nathaniel Robichaud. You were there to greet me with a smile the first day I joined the lab. That same day, you forwarded me a grant to get me off the ground to work on the first of four projects I would be part of in this lab, and since then, you have always been around for whatever help I may need. Thank you for everything – including translating the abstract into French.

I would like to thank my advisory committee members Jerry Pelletier, and Arnim Pause for their help in progressing my project.

I want to also like to acknowledgment and thank Daniela Quail for being my official thesis reviewer.

I would like to thank many lab members, as they provided friendship and insight, and helped create a supportive lab environment. It's a large lab, and there are many people to thank including: Mehdi Amiri, Clement Chapat, Sara Bermudez, Dana Pearl, Nadeem Siddiqui, Yuri Svitkin, Argel Aguilar-Valles, Edna Matta Camacho, Shane Wiebe, Jelena Popic, Agnieszka Skalecka, Mehdi Jafarnejad, Soroush Tahmasebi, Xu Zhang, Peng Wang, Chadi Zakaria, Sebastian Morales, Anmol Nagpal, Vijendra Sharma, Rapita Naresh Sood, and for your administrative assistance: Annamaria Kiss, Isabelle Harvey, Eva Migon, Annie Sylvestre, Meena

Vippariti and Annik Lafrance. Thank you Ritchie Truong and Sunghoon Kim for your help with the *de novo* Protein Synthesis experiments, and Colin Ratcliffe for your help with time-lapse microscopy.

Finally, I would like to express my appreciation to the Biochemistry Department, as well as McGill University.

LIST OF FIGURES

- Figure 1: Cellular viability assessment
- Figure 2: Proliferation in 2D
- Figure 3: Collective cellular migration
- Figure 4: Quantification of migration and invasion after 4 hr
- Figure 5: Representative images of migration and invasion after 24 hr
- Figure 6: Quantification of migration and invasion after 24 hr
- Figure 7: Representative images of time-lapse microscopy captured cellular migration
- Figure 8: Representative images of wound fluency
- Figure 9: Quantification of wound healing experiments
- Figure 10: Colony formation assessment after 24 hr of treatment
- Figure 11: Colony formation assessment after 72 hr of treatment
- Figure 12: SUnSET assay in cells
- Figure 13: SUnSET assay in tissue
- Figure 14: Timeline of experiments in NOG mice
- Figure 15: Results of experiments in NOG mice
- Figure 16: Timeline of experiments in BALB/c mice
- Figure 17: Results of experiments in BALB/c mice
- Figure 18: Tumor T cell infiltration
- Figure 19: Current understanding of data
- Figure 20: Appendix: comparison of 4T1 vs 4T1-luc cells in BALB/c mice

TABLE OF CONTENTS

Abstract.....	2
Resume.....	4
Quote.....	6
Dedication.....	7
Acknowledgements.....	8
List of Figures.....	10
Table of contents.....	11
Introduction.....	12
Rational and hypothesis.....	22
Significance.....	22
Methods.....	23
Results.....	32
Discussion.....	73
Appendix.....	78
References.....	79

CHAPTER 1

1.1 Introduction

There are approximately 20,000 genes capable of encoding proteins in every cell [1]. Protein abundance is under tight control within the body, particularly at the level of protein synthesis, as it accounts for ~1/3 of total energy consumption in differentiating mammalian cells [2]. Initiation of translation is a very regulated process [3], and control of mRNA translation is arguably the single most important mechanism of regulating gene expression [4]. Ultimately, transcription, translation and post-translational events all contribute to the regulation of gene expression [5].

Eukaryotic translation initiation factor 4E (eIF4E), eIF4G, and eIF4A compose the heterotrimeric protein complex eIF4F [6-11]. It is interesting to note that eIF4A is the most abundant translation initiation factor, while eIF4E is the least [12-14]. eIF4E binds to the cap of mRNA [10]. The cap structure is m⁷ G(5')ppp(5')N, with N being represented by any nucleotide [15, 16]. The rate-limiting step of eukaryotic translation initiation is the cap-binding protein eIF4E [16-18] due to its role in recognizing the 5' end cap of nuclear transcribed mRNAs [16, 19]. eIF4F recruits 40 S ribosomal subunits to the 5' cap of mRNA via interactions with eIF3 [11, 20, 21]. The 40 S ribosomal subunit is responsible for bringing with it the initiator methionine-tRNA to the 5' end [11, 21-23]. It then scans the mRNA toward the 3' directions looking for the start codon [22, 24]. Thus, after eIF4E recognizes the mRNA cap, the 40S ribosomal subunit together with the ternary complex and various initiation factors (eIF1, eIF1A, eIF3, and eIF5) forms the 43S pre-initiation complex (PIC) [25, 26].

Protein synthesis always begins with the amino acid methionine [27, 28], and the codon AUG [29]. Following this, the 60 S ribosomal subunit also joins [22, 23]. The 40 S and 60 S subunits join together at the initiation codon and now form the 80 S eukaryotic ribosome complex, which can decode the RNA to create a functional protein [22, 23, 30, 31].

The activity of eIF4E is controlled and regulated at multiple levels (mRNA and protein) to defend against cancer, including via eIF4E binding proteins (4E-BPs), which block eIF4E activity [32]. The majority of eIF4E is typically prevented from forming a complex with eIF4F via eIF4E binding 4E-BP1, under homeostatic/basal conditions [19]. This serves to prevent excessive cap-dependent translation [19]. 4E-BPs are controlled by the protein mechanistic target of rapamycin (mTOR), which phosphorylates 4E-BP1 at four serine/threonine residues [24]. This phosphorylation functions to impair 4E-BP1-mediated eIF4E repression [24], since hyper-phosphorylated 4E-BPs fail to bind to eIF4E, thus leading to elevated protein synthesis and uncontrolled cell growth [33, 34]. This is why many cancers such as prostate, breast, and melanoma display hyperactive mTOR signaling [35-39].

1.2 Translation & Cancer

The conventional thinking is that abnormal gene expression leads to cancer [40]. This can occur from a number of factors such as mutation, amplification, and/or deletion [40]. The multi-step development of a malignancy from a “normal” cell is termed tumorigenesis [41]. The original seminal papers by Hanahan and Weinberg defined in 2000 what they view as the hallmarks of cancer, including factors such as resistance of cell death, and the activation of invasion and metastasis. Among other recommendations, the 2011 update stressed the importance of cross-communication amongst tumor cells and their respective tumor

microenvironment (TME) [42]. Targeting translation is a viable strategy to target various hallmarks of cancer [43].

The main feature separating malignant cells (i.e. potentially metastatic) from those that are benign is the ability to be invasive [44]. During breast cancer, a primary tumor may remain confined to the lobules or milk ducts of the breast (referred to as ductal carcinoma in situ) [45]. On the other hand, an invasive cancer will begin to grow beyond the confines of the breast compartment in which it originated, becoming what is referred to as an invasive ductal carcinoma [45, 46]. Cancers typically require the ability for continuous and rapid growth [47], which means there is a necessity for elevated rates of translation [47]. Broadly speaking, translation is simply the mechanism by which genetic information moves from RNA and becomes a polypeptide chain [48], and there is an undoubted connection between neoplastic formation and translational disarray [48]. There has been a great deal of focus on modulating the role of translation initiation factors in protein synthesis, given that initiation is the most highly regulated, and rate-limiting step of this process [19, 49, 50].

Decades of research suggest that targeting protein synthesis in cancer could have therapeutic applicability [51], and points to the idea that multiple cancers might be susceptible to protein synthesis inhibitors [51]. Sidney Pestka discussed the potential use of translation inhibitors more than 40 years ago, where he highlighted the utility of antibiotics to learn about the mechanisms of translation [19]. eIF4E is a well-known proto-oncogene [52], and cancer cells are some of most privileged beneficiaries of elevated translation via eIF4F [53]. Furthermore, early experiments showed that NIH 3T3 and rodent fibroblast cells undergo malignant transformation upon overexpression of eIF4E, suggesting its potential to act as a potent oncogene

[16]. This was characterized by observing the appearance of foci *in vitro*, and the formation of tumours in immune-compromised mice [16]. There have been a multitude of therapeutic avenues aimed at inhibiting excessive mRNA translation, since it typically leads to increases in mRNAs that contribute to tumor formation and growth such as BCL-2, MCL-1, and c-MYC, among many others. In an attempt to curb this, many drugs targeting translation have been explored, and strategies have been aimed at the interaction of eIF4E with the cap, antisense nucleotides against eIF4E, as well as inhibition of eIF4G and eIF4A activity [54]. Given the diversity of mRNAs preferentially regulated, it is no surprise that eIF4F-mediated abnormalities have been linked to everything from cellular transformation and tumorigenesis, to therapeutic resistance [55]. Another avenue being approached clinically is the utilization of combination therapy targeting both metabolism and translational dysregulation in cancer [55].

Although previous studies have focused on a wide range of cancer types, melanoma is an attractive target in translation research. It has been demonstrated that melanoma proliferation and invasion is reduced after either eIF4A or eIF4E are silenced [56]. In addition, this paper made a very interesting discovery, whereby when eIF4A1 and eIF4E are depleted via siRNA only 19% of all affected proteins depleted were shared in common in their melanoma models [56]. This suggests that melanoma is an important cancer target that should be the focus of research of both anti-eIF4E therapy, and a target of small molecule inhibitors against eIF4A. Furthermore, this study went on to demonstrate that cell cycle targets of both eIF4A and eIF4E are correlated with patient survival in specimens taken from melanoma patients [56].

Breast cancer is perhaps the disease that has the most amount of currently available research, and clinical implications suggesting that it is an attractive target for translation

inhibition. There is data to demonstrate that knockdown of eIF4E is effective in TNBC [57]. In addition, a recent paper from the Sonenberg lab demonstrated a pro-metastatic role for phosphorylation of eIF4E in murine breast cancer metastasis [58]. This builds on previous research which demonstrated that inhibition of phosphorylated eIF4E (utilizing MNK inhibitors) could be effective in reducing breast cancer proliferation and survival [59]. This evidence points to an important role for both phosphorylated eIF4E, and eIF4E in breast cancer. However, less is known about the role of eIF4A in breast cancer. Modelska et al., recently presented strong evidence that eIF4A can serve as an independent predictor of outcome in breast cancer patients [60]. This was also supported by pre-clinical research suggesting that murine tumors in an immune-compromised setting can be effectively treated with an eIF4A inhibitor [61].

It is becoming increasingly evident that the TME plays a vital role in a plethora of various cancers. There has been some inquiry into the role of mRNA translation in the context of the TME, although it still requires additional research. One important factor in the TME are chemokine receptors. Indeed, the chemokine receptor CCR5 (and its ligand CCL5) were sensitive to treatment by the mTOR inhibitor rapamycin in a breast cancer setting [62]. Furthermore, the same group showed that CCL5 plays a role in priming CD4⁺ T cells to undergo the process of chemotaxis in response to rapamycin treatment [63]. Rapamycin and other mTOR inhibitors are well-known for their immunosuppressive properties such as their ability to reduce T cell proliferation [64]. This has hampered their use in immune-competent settings, but the hope is that targeting downstream of mTOR (i.e. the eIF4F complex) could help mitigate drug resistance and potentially immunosuppression. However, as discussed below, this may not be the case. On the other hand, mTOR inhibitors have continued to receive interest given that they can provide chemotherapeutic sensitization in a TNBC and colon cancer models, providing a rational

for their use as a possible therapeutic agents as long as their effect on the TME is explored [65, 66]. The problem with this type of approach can be at least partly attributed to the induction of T regulatory cells (Tregs), which are pro-tumorigenic [67], and appear to be activated by mTOR inhibitors [67-69]. Thus, the activity of mTOR in T cells serves as an important signalling hub and senses changes in the TME [70]. Treg cells are able to utilize environmental signals to facilitate changes in gene expression via Foxp3 [71]. After thorough translome analysis, it has been demonstrated that suppressing eIF4E specifically in Foxp3- CD4+ T cells leads to an increase in Foxp3 protein levels, suggesting that eIF4E is involved in regulating T cell differentiation. In addition, this paper suggests that when eIF4E is inhibited (under activating conditions) there is an increase in differentiation of Foxp3- CD4+ T cells towards induced Tregs, particularly since Foxp3 is a well-known marker of essential lineage-commitment [72, 73]. It remains to be established if the eIF4F complex plays an equally important role as mTOR in the TME, particularly in a cancer setting.

This aforementioned research should at very least underscore the important role that the interplay between mRNA translation and the TME in cancer initiation and progression. Some of this research was performed in either cell culture models, or in immune-compromised mice. It would thus be very relevant and interesting as to how this could potentially differ in an immune-competent, and TNBC setting (this is relevant to the data and discussion below).

1.3 Premise for the use of Translation Inhibitors

Vital to the entire premise and fortitude of using translation inhibitors, is evidence demonstrating that there is a great amount of selectivity in the mRNAs which rely upon eIF4F

[74-76]. This is mostly owing to the secondary structure in the 5' untranslated region (UTR), with the length and structural complexity being the main determinants of this [74]. Efficacy of translation can in part, be dictated by the amount of 'complexity' of secondary structures within the 5' UTR [3]. Critically, these eIF4F-sensitive mRNAs and those that are overwhelming involved in tumorigenesis, cancer, and metastasis. This underpins much of the reasoning for directly targeting translation as an anti-cancer therapy. eIF4A is particularly important, as cell-free *in vitro* translation assays demonstrate that the existence of secondary structures, and the degree of mRNA secondary structure is directly proportional to the amount of eIF4A that is needed to unwind them [74]. Thus, more stable secondary structures actually decrease translational efficiency (ribosome scanning), and require more eIF4A [77]. Further, proof-of-concept experiments demonstrated that dominant-negative mutant eIF4A (alanine substitutions of motif Ia) differentially inhibit the translation of these mRNAs [74]. Work from the Sonenberg lab has also demonstrated that mRNAs with structured UTRs were especially targeted when eIF4E was experimentally overexpressed [78]. In addition, many facets of tumour biology such as migration, invasion, metastasis, and treatment resistance are intimately influenced by mRNA translation [55, 79, 80]. Thus, house-keeping proteins such as β -actin, which have short and relatively unstructured 5' UTRs are referred to as strong mRNAs, are efficiently translated [81, 82]. Conversely, many oncogenes are described as weak mRNAs, and display long and structured 5' UTRs, with evidence demonstrating that they are uniquely responsive to translation initiation [81, 83].

1.4 Targeting eIF4A

Perhaps the most important role that eIF4A plays is as a classical RNA helicase, where it belongs to the DEAD box family [74]. It unwinds secondary structures in the 5' UTR [24], allowing for efficient translation of selective mRNAs in conjunction with other helicases [3]. As mentioned, unwinding secondary structures is critical for efficient scanning by the ribosome until it reaches the start codon [24]. mRNAs with relatively minimal secondary structures still require eIF4A helicase activity [84], and eIF4A-mediated RNA unwinding appears to be necessary for ribosome recruitment even for mRNA with few secondary structures. Dysregulated eIF4A activity has been linked to various types of cancers including breast [60], and T-cell acute lymphoblastic leukaemia (T-ALL) [85]. The translation of mRNAs with 5' UTRs that possess the ability to form G-quadruplexes is an important mechanism of action whereby eIF4A functions as an oncogene [60, 85]. Importantly, Modelska et al. recently demonstrated that 5' UTRs with a high content of G/C are preferentially translated by eIF4A [60], and patient lung carcinoma samples display elevated protein levels of eIF4A [86].

Historically, the use of small molecular inhibitors have provided a wealth of information regarding various steps of the protein synthesis pathway [51]. Using small molecules to inhibit biological processes has distinct advantages, such as allowing for quick onset of action, and provides information that could not be probed using genetic methods [51]. eIF4A can exist in two conformations (active or inactive), to allow for ATP-mediated mRNA unwinding [24]. Thus, it can be assumed that increasing the amount eIF4A that is in the inactive state would be beneficial as an anti-cancer strategy. Hippuristanol is one such small molecule which displays this mechanism of action, locking eIF4A in this conformation [24].

Another inhibitor, Pateamine A, does not target the helicase activity of eIF4A directly, but instead disrupts its interaction with eIF4G, which nonetheless leads to reduces translation (in some case more than 20-fold), and does not depend on 5' UTR length [87, 88].

There are in fact many names to describe a similar in function branch of eIF4A inhibitors distinct from Hippuristanol and pateamine A. Silvestrol is perhaps the most interesting compound from this flavagline family, which are part of a chemical class of cyclopenta[b]-tetrahydrobenzofurans, which also go by the name rocaglamide and include compounds such as Rocaglamide-A (Roc-A) [61, 89, 90]. Previous work has already addressed the role of silvestrol in protein synthesis alterations [85, 91], demonstrating that mRNAs that are particularly sensitive to silvestrol are those with long and structured 5' UTRs, which actually corresponds to < 300 transcripts [91]. Furthermore, the 5' UTRs of silvestrol-sensitive mRNAs are enriched for G-quadruplexes [91]. Importantly, a multitude of oncogenes are encoded by mRNAs that are preferentially targeted by silvestrol treatment [91]. Surprisingly, silvestrol actually *increases* the binding of eIF4A to mRNA [61]. Large quantities of silvestrol are difficult to synthesize given its complex structure. Thus, synthetic derivatives such as CR-1-31-B have been developed.

1.5 Targeting eIF4A instead of eIF4E

An elegant study by Feoktistova et al., revealed that through eIF4G-mediated conformational alterations eIF4E actually increases the helicase activity of eIF4A, as it was shown to prevent auto-inhibition via eIF4G thus relieving the suppression of eIF4A [25, 81]. This would suggest that in addition to its well-established role in cap-binding, eIF4E can also stimulate the helicase activity of eIF4A, making it an attractive target. The results of clinical trials, however, have not been particularly encouraging [92]. This phase I/II clinical trial recently conducted using eIF4E-specific antisense oligonucleotides (ASO) utilized as a combination therapy together with irinotecan [92]. This trial utilized a second-generation ASO (ISIS 183750), leading to a discernible reduction in tumor-specific eIF4E RNA. It is possible that increased efficacy, particularly at the protein level, might be achieved with increased therapy duration [55]. Furthermore, a recent paper from the Topisirovic lab provided invaluable knowledge as to the difference in targeting eIF4E and eIF4A [93]. They demonstrated that drugs targeting eIF4A lead to cytotoxicity. However, as opposed to eIF4E, inhibition of eIF4A leads to decreases in the synthesis of the proteins that maintain mitochondrial integrity, but not those that effect proteins influencing mitochondrial activity. This leads to a cytostatic effect when inhibiting eIF4E, while eIF4A inhibition ultimately causes cytotoxicity [55, 93, 94].

Furthermore, the role of translational control in the TME is a relatively unexplored area of research. The Sonenberg lab has begun to map out the role that translation plays here, but the focus has so far been on eIF4E and its phosphorylation. Our recent paper utilizing eIF4E knock-in mice, demonstrated that phosphorylation of eIF4E either within cancer cells themselves, or within their corresponding TME actually promotes metastatic burden [58]. This

study demonstrated that although primary tumor growth as a result of orthotopic murine mammary tumor injection (66cl4) and the resulting immune infiltration were comparative, mice that cannot phosphorylate eIF4E (due to a ^{S209A} mutation) had significantly less lung metastasis as compared to their WT counterparts. This paper also provides the first evidence that targeting components of the translational pathway influence the TME, as the mutant eIF4E mice displayed less pro-metastatic neutrophils [58]. However, although these results were very encouraging, as previously mentioned, clinical trials targeting eIF4E have not been particularly impressive, which suggested to us that in addition to exploring the role of eIF4E in this domain, it would be pertinent to assess the efficacy of eIF4A inhibition. Thus, we noticed that there is a knowledge gap, whereby one of the critical components of cap-dependent translation has received a relatively small amount of attention for its potential influence in cancer and metastasis. In particular, not much is known about the role that eIF4A plays in metastasis, and in various immune cell types. We were principally trying to treat TNBC, which is the deadliest form of breast cancer, and wanted to utilize a small molecular inhibitor that has previously demonstrated efficacy in multiple (mostly immuno-deficiency) cancer settings.

RATIONAL

There is a particular lack of experimental data addressing the question of how translation inhibitors effects the TME. The vast majority of previous studies utilized immune-compromised mice when testing the effects of various translation inhibitors. Thus, we wanted to establish the role of an eIF4A inhibitor in a TNBC cell line, and then to compare the effects of treating established tumors in different host immune systems i.e. immune-compromised NOD/Shi-

scid/IL-2R γ ^{null} (NOG) mice, and immune-competent BALB/c mice. Delving into any potential differences in response can help us address this relatively unknown area of research.

HYPOTHESIS

We hypothesize that treating TNBC cells with low nanomolar concentrations of an eIF4A inhibitors will lead to significant reductions in markers of metastasis *in vitro*, and will markedly reduce the formation of primary tumors in mice.

SIGNIFICANCE

The link between initiation factors such as eIF4E and cancer has been extensively studied for over three decades. However, the role of eIF4A has received much less attention. Furthermore, there existed a need to look more in-depth at the role of eIF4A inhibition on metastasis. In addition, the role of translation inhibition in the tumor microenvironment is essentially unknown. Various inhibitors have been gaining popularity, given that they display profound cytotoxicity (nM range) in many types of cancers, and lead to significant reductions (or prevention) of tumors in immune-compromised mice. This study demonstrates the previously unappreciated role of the adaptive immune system has in influencing the efficacy of translation inhibitors. The data suggests, that at least in certain situations, translation inhibitors can have detrimental effects on certain immune populations, and that perhaps, combination therapy together with translation inhibitors is the more favourable way forward. This hypothesis remains to be explored, but represents a very exciting area of research.

METHODS

Cell Culture

The 4T1 and 4T1-luciferase expressing TNBC cells were a kind gift from Dr. Peter Siegel (McGill University). 4T1 cells are originally derived from the mammary gland of BALB/c mice, and thus are syngeneic for BALB/c mice. It is an adherent cell line displaying epithelial morphology, and is used to model TNBC. They are also compatible with a range of immunocompromised mouse strains such as nude, NSG, and NOG. B16 cells were purchased from ATCC, and are an excellent melanoma model. B16 cells are an adherent cell line displaying a morphology that is a mix of both epithelial and spindle shaped cells. They were originally derived from a C57BL/6J mouse background. Both cells were cultured at 37°C with 5% CO₂ in either RPMI-1640 medium (Sigma-Aldrich) for 4T1 cells, or in DMEM medium (Sigma-Aldrich) for the B16 cells. Medium was supplemented with 10% FBS, and 1% P/S. These cell lines were chosen because they are syngeneic in two types of mouse strains - 4T1 in BALB/c, and B16 in C57BL/6J, thus allowing use to test the role of eIF4A inhibition in two separate mouse backgrounds. These cells were also chosen to allow us to assess the efficacy of our inhibitor in a TNBC and melanoma model. Finally, it is well established that both cell lines metastasize, thus providing us the ability to really elucidate the role of eIF4A inhibition in the process of metastasis.

Animal Studies

1 x 10⁵ cells were injected into the second mammary fat pad of BALB/c mice, and for other sets of experiments into the same location in NOG mice. BALB/c mice were bred in house,

and NOG mice were purchased from Taconic Biosciences, Inc. NY, US. All of the mice used in our experiments were female, and were between eight and twelve weeks of age. Some experiments utilized parental 4T1 TNBC cells, while others utilized 4T1 luciferase (luc)-tagged 4T1 cells. The purpose for using 4T1-luc cells was to allow for bioluminescence imaging (BLI). As has recently been reported however [95, 96], luciferase, especially when tagged to 4T1 cells, induces an immune response resulting in smaller tumours, thus preventing us from adequately assessing metastatic burden. Our own in-house experiments recapitulating some important aspects of this recent paper (shown in the appendix). Tumors were measured every three days via caliper measurements. Mice were also weighed with the same frequency, to assess for overt signs of toxicity and/or potential ethical issues such as hunched back or dehydration. Mice bearing tumors were dosed I.P. with vehicle (5.2% PEG400/5.2% Tween80), or CR-1-31-B (0.2 mg/kg), daily for 14 days.

Tumor volume was estimated at the indicated time points using the formula $V = \frac{4}{3} \times (3.14159) \times (\text{Length}/2) \times (\text{Width}/2)^2$ and caliper measurements of the longest and shortest diameters of the tumor, as was previously done in our lab [58]. After mice were euthanized, their organs (lungs, livers, and spleens) along with their tumors were immediately fixed in 10% formalin for 24 hr, followed by embedding in paraffin for downstream analysis such as immunohistochemistry (IHC). All experiments involving animals were conducted in accordance with McGill University animal care guidelines (McGill University and Affiliated Hospitals Research Institutes Animal Use Protocol #2011-4076).

Cellular Viability

Measurement of cellular viability was performed using the Cell Counting Kit-8 (CCK-8) assay, which is manufactured by Dojindo Molecular Technologies Inc. The CCK-8 assay utilizes the water-soluble tetrazolium salt [2-(2-methoxy-4-nitrophenyl)-3-(4-nitrophenyl)-5-(2,4-disulfophenyl)-2H-tetrazolium (WST-8) [97, 98]. Colorimetric changes representing cellular viability are assessed by the reduction of WST-8 via cellular NADH dehydrogenases, with 1-Methoxy PMS acting as an electron mediator, ultimately producing an orange colored formazan dye. This color is representative of cellular dehydrogenase activities, and correlates with the amount of viable cells [99]. 4T1 cells were allowed to adhere onto 96-well plates overnight. CCK-8 (Dojindo Molecular Technologies Inc. Burlington, ON, Canada), was then added to cells, and incubated in the dark for 2 hours. Optical density was read spectrophotometrically at 450 nm.

Cellular Proliferation

Measurement of cellular proliferation was assessed in a 2D environment. Assessment of 2D proliferation (standard cell culture conditions). 5×10^3 4T1 cells were seeded in 6-well plates. After allowing cells to adhere overnight, cells were treated with either DMSO or increasing concentrations of CR-1-31-B for up to 96 hr. Cells were immediately inserted into an Essen Biosciences cell imager, and incubated at 37°C. Images were taken every 2 hours providing live-cell imaging (IncuCyte; Essen Biosciences), and quantified using IncuCyte software [100].

Collective cell invasion assay

In separate experiments, 4T1 and B16 cells were treated with CR-1-31-B (1 – 200 nM). After 24 hr the cells were trypsinized, counted, and 2×10^3 cells were then seeded in 96-well plates, into 50 μ L of 50% growth factor-reduced matrigel, and incubated at 37°C for one week. The cells were directly resuspended and plated within the matrigel. This assay allows for visualization of cellular morphology and colony outgrowths in matrigel, which represents the invasive potential of the cells, whereby it is meant to approximate the likelihood that they will penetrate through the basement membrane. The end-point measurement is strictly qualitative, and is used to assess invasive potential in a 3D environment [101, 102].

Migration & Invasion

Migration of cells was assessed using BD Biosciences (Franklin Lakes, NJ, USA) 24-well cell culture inserts to be utilized as a Boyden chamber. This type of set-up allows for the measurement of directed cell migration [103]. Cells were trypsinized, and then 250,000 cells were plated into the upper portion of the insert, after being resuspended in serum-free media as previously reported [101]. Cell migration is stimulated by adding 10% serum to the lower chamber, and incubated for the indicated time periods, in the presence or absence of various concentrations of CR-1-31-B (1 – 200 nM). The same protocol was followed the invasion assay, except the inserts were pre-coated for one hour with 50 μ L of 5% (in media) growth-factor reduced matrigel (BD Biosciences). After the indicated time points (either 4hr or 24hr), all media is aspirated, inserts are washed twice with PBS. The inserts are then fixed via 4% paraformaldehyde in 1x PBS for 20 min, and stained with crystal violet (0.2%) in 1x PBS for 20 min. This is followed gently dunking the insert into ddH₂O, and carefully removing excess

crystal violet from the upper part of the cell culture insert with a cotton tipped applicator. The crystal violet dye is used since it is known to bind to proteins and DNA [104], and will thus help to assess the amount cells that have migrated through the BD Biosciences cell culture insert, and help differentiate them from dead cells and potential debris. The cell cultures are allowed to dry at RT overnight. The following day, a standard method was employed for quantification of cellular migration and invasion (through matrigel) [105, 106]. For both the migration and invasion experiments, cells that had migrated through the porous membranes of the cell culture insert were manually quantified in five random fields chosen at 20x magnification.

Scratch/Wound Assay

Collective cellular migration measurements were performed using a classical scratch/wound assay [107, 108]. Fibronectin (0.01mg/ml, Sigma F1141) was diluted in PBS, and was added to Essen ImageLock 96-well plates (Essen Bioscience, Ann Arbor, Michigan, USA) at 37°C for 30 min, to help prevent cell detachment following wounding. Fibronectin was then aspirated, washed once with PBS and allowed to dry for 1 hr. Afterwards, 4T1 cells were plated and allowed to adhere overnight. The following day, the plate is washed twice with PBS, and after PBS is removed, media containing DMSO or various concentrations of CR-1-31-B (1-200 nM) for up to 24 hr is added. For some experiments, cells were pre-treated with 10µg/mL mitomycin C (for 2 hr) in order to help exclude the effects of decreases in proliferation caused by CR-1-31-B, and to instead quantify only the decrease in collective cell migration. The plate is incubated inside of an IncuCyte for 24 hr, and all images are taken at specified time points (every 2 hr), at the same location, and wound closure is then analyzed and quantified using IncuCyte™ software (Essen Bioscience).

Western Blotting

For *in vitro* experiments, cell monolayers were washed twice with ice cold phosphate-buffered saline and harvested using trypsin. The cells were then pelleted and lysed in homogenization buffer containing: 50 mM Tris·HCl (pH 8 at 4°C), 1 mM EDTA, 10% (wt/vol) glycerol, 0.02% (wt/vol) Brij-35, 1 mM DTT, and protease and phosphatase inhibitors (Sigma). The lysates were then centrifuged at 12,000 g for 10 min [109]. The protein concentration was then measured using the Bradford method utilizing a Bio-Rad protein assay dye reagent concentrate (Bio-Rad, Mississauga, ON, Canada). Equal parts of protein and Laemmli sample buffer were mixed and boiled for 5 minutes, and separated by SDS-PAGE. Following electrophoresis to nitrocellulose membranes, Ponceau Red Staining was employed to confirm equal loading of protein. The membranes were blocked in 10% skim milk for one hour, and incubated overnight with primary antibody diluted in 5% BSA at 4°C. After extensive washing (3 x 10min using TBS-T), the membranes were incubated for 1 hr with horseradish peroxidase-conjugated secondary antibody (diluted 1:1000 in TBS-T). Membranes were developed with chemiluminescence Plus Western Blotting Substrate (Roche). Signals were quantified using Image J software (NIH, Bethesda, MD, USA). The primary antibody against β -actin was purchased from Cell Signalling Technology. Anti-puromycin monoclonal antibody (3RH11) was purchased from KeraFast.

For animal experiments, frozen liver tissue extracts from eight to twelve week-old female BALB/c mice were prepared in ice cold homogenization buffer containing: 20 mM Tris-HCl, pH 7.4; 150 mM NaCl; 1 mM EDTA; 1% Triton, 5 mM NaF; 1.5 mM Na₃VO₄, and protease inhibitor cocktail (complete, EDTA-free, Roche Applied Science). The remaining protocol steps were the same as that which were used for *in vitro* samples.

Colony Formation

Cells were seeded in 6-well plates and allowed to adhere overnight. The following day, cells were treated with various concentrations of CR-1-31-B or DMSO for either 24 or 72 hr, to provide an indication of a relatively short and long-term response to treatment. Following this, cells were gently trypsinized, carefully counted using trypan blue and a hemocytometer, and 1000 cells were seeded in 10 cm plates. Cell culture media was refreshed every three days. After one week, cell culture media was removed, and plates were carefully washed twice with PBS. Cultures were then fixed with 1% formaldehyde and 1% methanol in dH₂O, and stained with crystal violet (0.5% w/v) for 20 min at RT. Colonies (>50 cells) were then counted and quantified using an inverted microscope.

Measurement of *de novo* Protein Synthesis

Eight to twelve week-old BALB/c mice bearing palpable (via caliper) 4T1-luc tumors were injected intraperitoneally (I.P.), into the mammary fat pad in parallel with vehicle (5.2% PEG400/5.2% Tween80) or CR-1-31-B (0.2 mg/kg) for 1 h. Following this, they were injected with puromycin at 10 mg/kg, I.P., and 1 h later livers were collected and processed for Western blotting, using anti-puromycin monoclonal antibody (3RH11). Membranes were developed with chemiluminescence Plus Western Blotting Substrate (Roche). The unlabelled protein control was subtracted from the total signal for each lane (15 – 250 kDa) to determine protein synthesis. Image J software (NIH, Bethesda, MD, USA) was then used to quantify the signals.

Immunohistochemistry

Tumors that had been previously fixed in formalin and embedded in formalin were rehydrated by 5 min washes in xylene x 3, followed by two washes with 100% ethanol, one wash with 70% ethanol, and finally, 5 min of running tap water, and 2 min in ddH₂O. Antigen retrieval was performed by utilizing a citrate buffer (pH 6), and heating within a pressure cooker for 15 min, and cooled at RT for 1 hr, as previously done [58]. Tumor sections were then washed with PBS (2 x 5min) and blocked in 2.5% normal horse serum (10 min), and incubated with primary antibodies (in 2.5% normal horse serum) overnight. After PBS (2 x 5 min) washes, the endogenous peroxidases were quenched with 3% H₂O₂ in PBS for 5 min. This was followed up by PBS washes (3 x 5 min) and incubation with HRP-conjugated ImmPRESS secondary antibodies (30 min), and 3 x 5 min PBS washes. The slides are then incubated with DAB (20 sec) and counterstained with 20% hematoxylin (30 sec). Images are taken using Aperio ImageScope software. All reagents were from Vector Labs.

Statistical analyses

The specific statistical tests are indicated in the figure legends. These were either Unpaired Student's T-test (when comparing two items) or for some experiments we performed a 1-way or 2-way ANOVA (more than three groups and singular or multiple parameters) followed by a Bonferroni Post-Hoc test. For tumor initiation experiments presented in the appendix, P values were calculated using the Mantel-Cox method. For replicate values data are presented as S.E.M. Two-sided tests were utilized, and statistical significance was achieved when $p < 0.05$. GraphPad Prism7 software for used for all statistical analysis.

3. RESULTS

3.1 CR-1-31-B reduces cellular viability

Previous work has shown that eIF4A inhibitors have cytotoxic effects towards various cancer cell lines [93, 110, 111]. We therefore wanted to assess the potency of CR-1-31-B in our system (4T1-luc cells). We observed a concentration and time-dependent decrease in cellular viability in our 4T1-luc cells upon treatment with CR-1-31-B. The half maximal inhibitory concentration (IC_{50}) was calculated as it provides an assessment of how much of a drug is needed to induce a 50% reduction in viability. This was calculated after 24 hours of treatment, and came out to ~10 Nm (Figure 1). This concentration is in agreement with previous reports utilizing eIF4A inhibitors in a cancer setting, such as hepatocellular cancer and nasopharyngeal carcinoma [112, 113]. This provided the first sign of *in vitro* evidence that CR-1-31-B can be effective in a TNBC setting.

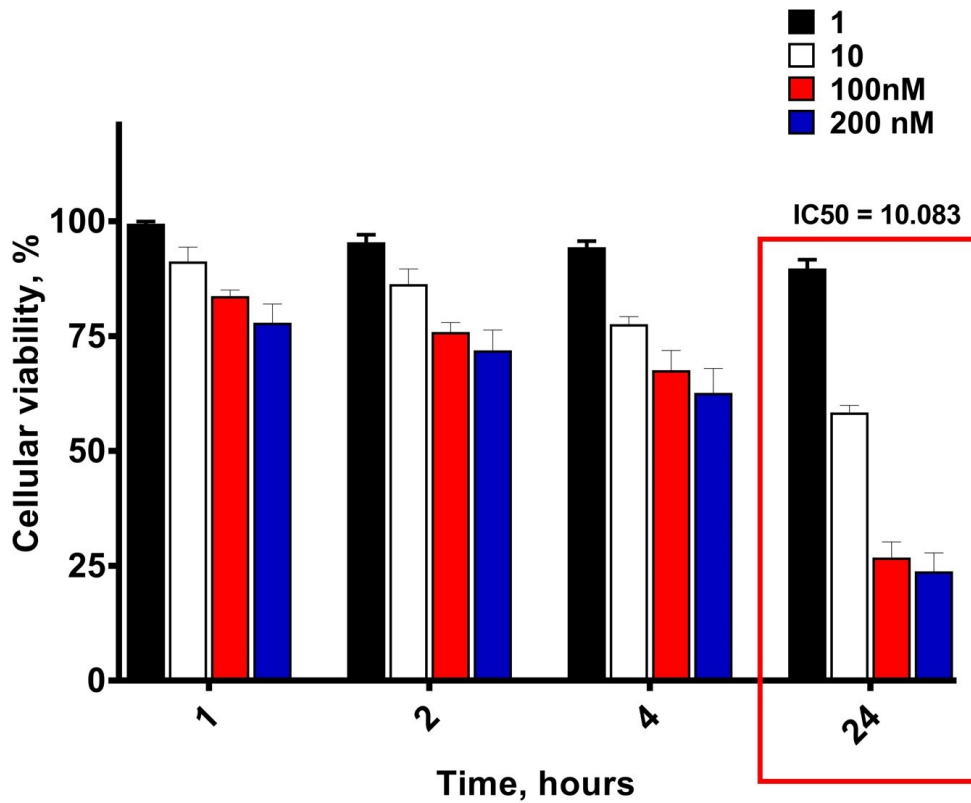


Figure 1: Quantification of cellular viability in 4T1 cells treated with CR-1-31-B (1 – 200 nM). Time and concentration-response over a 24 hr period is shown. IC 50 was calculated after 24 hr of treatment.

N=2. Data are mean \pm SEM

3.2 CR-1-31-B inhibits cell proliferation

Given the decrease in cellular viability that we observed with CR-1-31-B treatment, we next wanted to assess if this compound could also reduce proliferation of 4T1-luc cells *in vitro*, given the important role that cellular proliferation plays in both the development and progression of cancer [114, 115]. CR-1-31-B treatment in 4T1-luc cells led to a concentration and time-dependent decrease in proliferation over a period of 96 hr (Figure 2).

This decrease in proliferation is not unexpected since Rocaglamide A, which is a member of the eIF4A inhibiting rocaglate family, was recently demonstrated to inhibit Rac1 in HeLa cells [90]. Furthermore, Rac1 is an important protein for the proliferation of various cancers, and has been shown to be overexpressed and linked to increased aggressiveness in breast cancer [116-118]. Our observation of decreased proliferation in response to CR-1-31-B treatment, suggests that this compound has *in vitro* anti-cancer activity against TNBC.

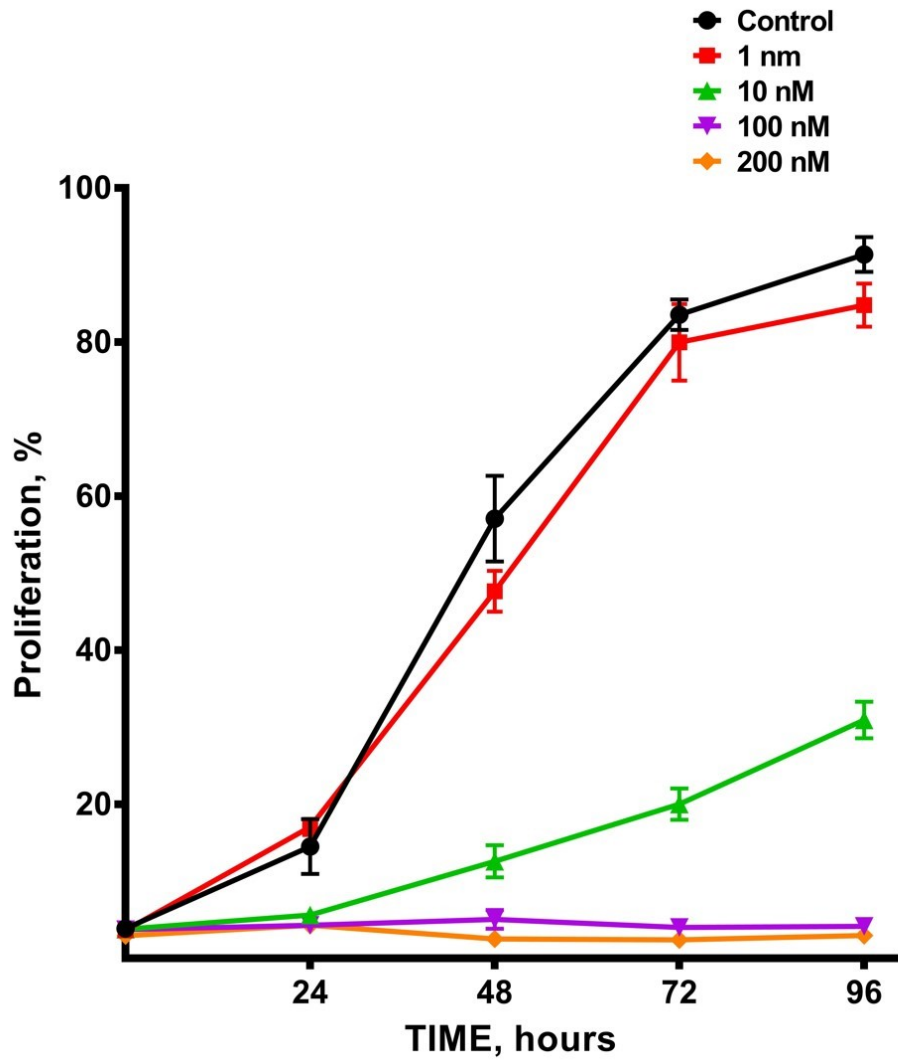


Figure 2: Quantification of cellular proliferation in 4T1 cells treated with CR-1-31-B (1 - 200 nM).

Time and concentration-response over a 96 hr period is shown.

N=2. Data are mean \pm SEM

3.3 Collective cell invasion is inhibited by CR-1-31-B treatment

The vast majority of cancer deaths in breast cancer occur as a result of metastasis, and not the primary tumor [119]. This is why doing an in-depth exploration of how a compound effects cellular migration and invasion in various conditions and assays is vital to perform. To this end, we performed a 3D collective cell invasion assay. Collective cellular invasion can occur when a group of cells cooperatively invade in various forms or patterns, such as cell clusters [120-122].

We found that a single treatment with CR-1-31-B led to a stark qualitative reduction in collective cellular invasion of 4T1-luc cells resuspended in matrigel prior to seeding (Figure 3 A-E). A very similar pattern was observed in CR-1-31-B treated B16 cells (Figure 3 F - J). These results provide a stark visual representation that eIF4A inhibition is effective in preventing collective cellular invasion in both TNBC and melanoma models.

4T1 Cells

B16 Cells

A

B

F

G

C

D

H

I

E

J

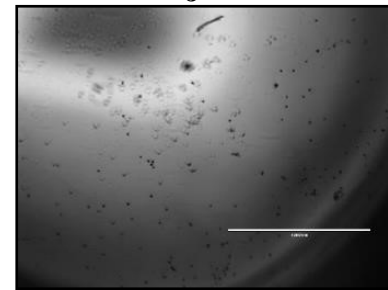
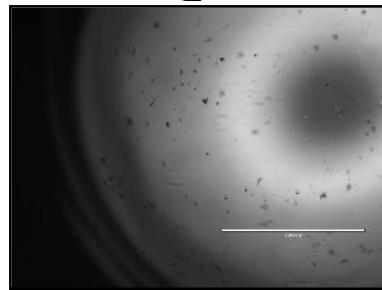
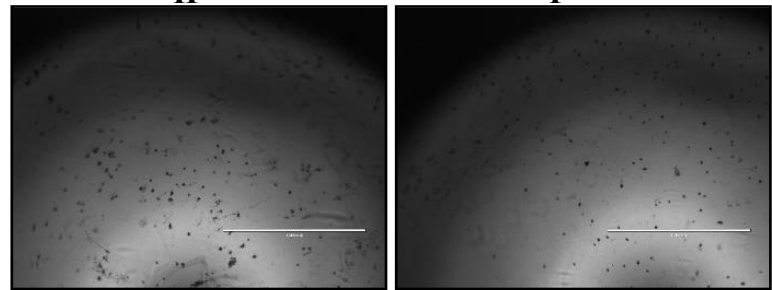
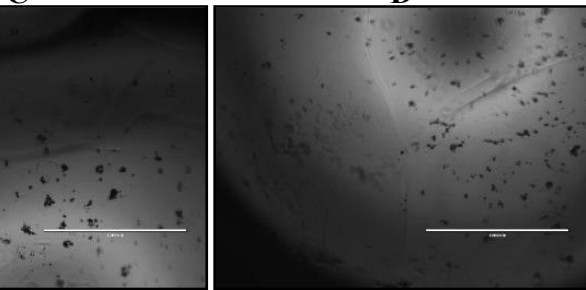
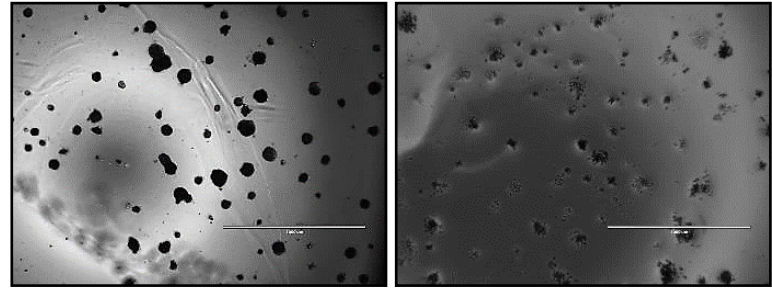
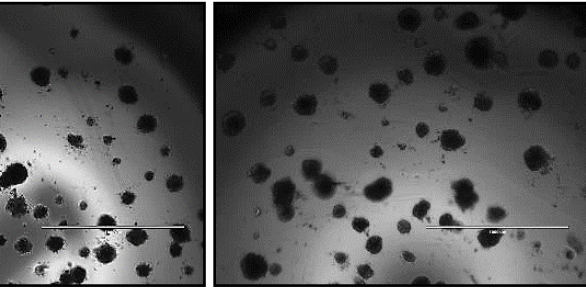


Figure 3: Representative images of three replicate experiments of colony outgrowth (invasive potential). Morphology of colonies growing from cells seeded in 50% matrigel, followed by 7 days of incubation. Images taken at 10X. **(A)** 4T1 cells control, **(B)** 4T1 cells 1 nM CR-1-31-B, **(C)** 4T1 cells 10 nM CR-1-31-B, **(D)** 4T1 cells 100 nM CR-1-31-B, **(E)** 4T1 cells 200 nM CR-1-31-B. **(F)** B16 cells control, **(G)** B16 cells 1 nM CR-1-31-B, **(H)** B16 cells 10 nM CR-1-31-B, **(I)** B16 cells 100 nM CR-1-31-B, **(J)** B16 cells 200 nM CR-1-31-B. N=3 (no statistics as this is a qualitative rather than a quantitative type of assay).

3.4 CR-1-31-B reduces cellular migration and invasion in TNBC and melanoma cells

We wanted to demonstrate that inhibition of eIF4A with CR-1-31-B could reduce *in vitro* measures of cellular migration and invasion. As opposed to the collective cell invasion assessed previously (see Figure 3), here, we are looking at single cell invasion, as well as migration. We utilized the classical transwell assay, which utilizes a Boyden chamber [103]. Boyden chambers are the gold standard for *in vitro* assessment of cellular migration and invasion [123]. At the most basic level, the Boyden chamber assay is simply two partitions separated by a microporous membrane [103]. For cancer therapeutics to be truly effective, they need to not only reduce viability and proliferation, but they must also have a direct effect on cancer cell migration and invasion. This type of assays allows for this type of assessment. Along these lines, observed changes cannot be just a change in proliferation, as the cells must first digest the artificial extracellular matrix (i.e. matrigel) before migrating allowing for better recapitulation of the *in vivo* cancer environment.

After just four hours of treatment with CR-1-31-B, we saw a decrease in migration and invasion of both 4T1 TNBC cells and B16 melanoma cells (Figure 4). Similar experiments were also performed, with the assessment occurring after 24 hr of CR-1-31-B treatment. Figures 5A - E provides representative images of changes in 4T1 cell invasion, while Figures 5F - J are representative images of changes in B16 cell invasion. We saw significant decreases in both cellular migration (Figure 6A) and cell invasion (Figure 6B) in 4T1 cells treated for 24 hr with CR-1-31-B. A very similar pattern was seen in cell migration and cell invasion of B16 cells treated for 24 hr with CR-1-31-B (Figure 6C and 6D). This provided us with important initial evidence that this compound could be very effective in reducing cellular migration in multiple cancer models.

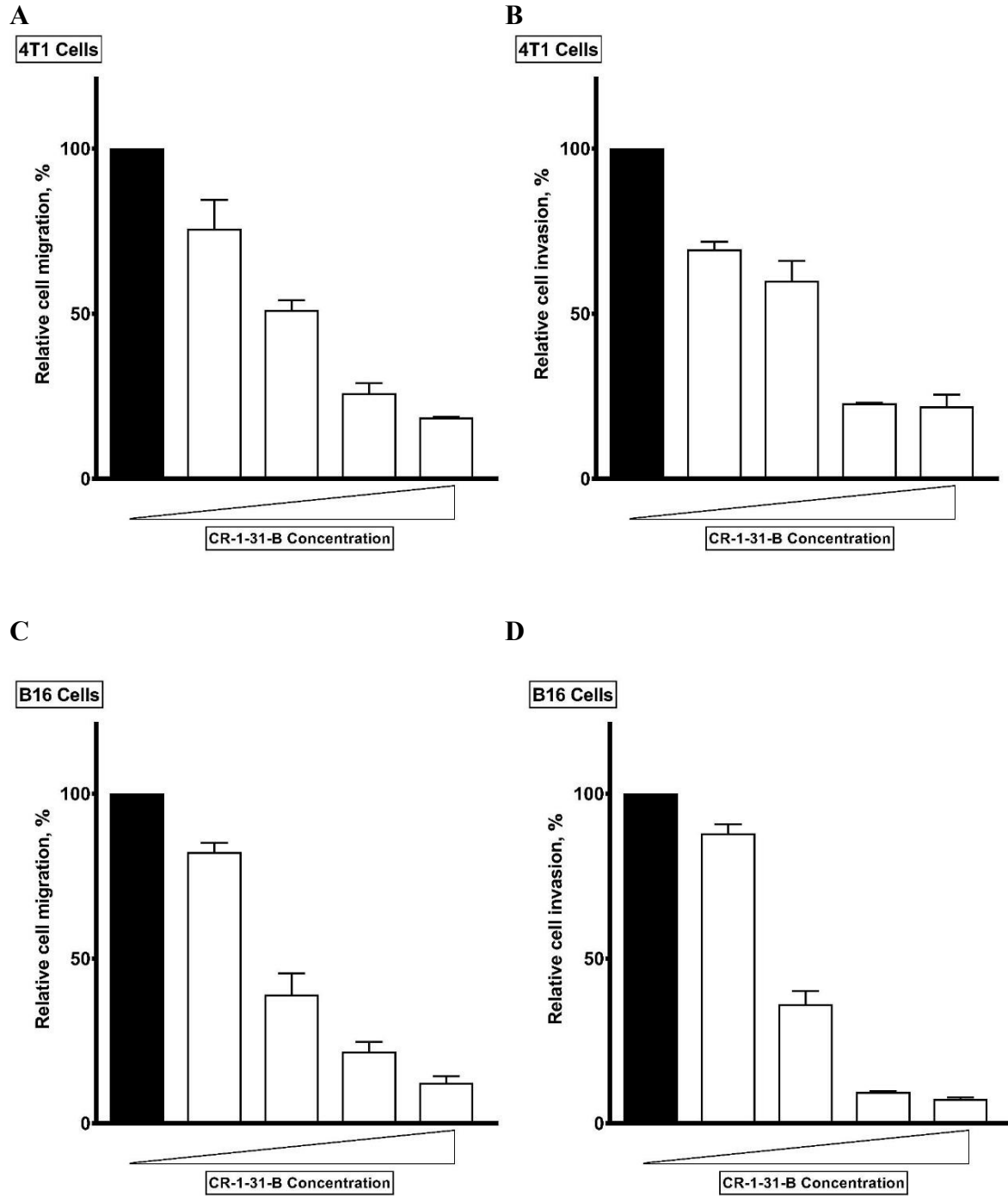


Figure 4: Quantification of Boyden chamber migration and invasion at 4 hr. Concentration-response (1-200 nM) or CR-1-31-B in 4T1 and B16 cells. (A) Migration of 4T1 cells treated with 1-200 nM of CR-1-31-B (B) Invasion of 4T1 cells treated with 1-200 nM of CR-1-31-B (C) Migration of B16 cells treated with 1-200 nM of CR-1-31-B (D) Invasion of B16 cells treated with 1-200 nM of CR-1-31-B N=2. Data are mean \pm SEM

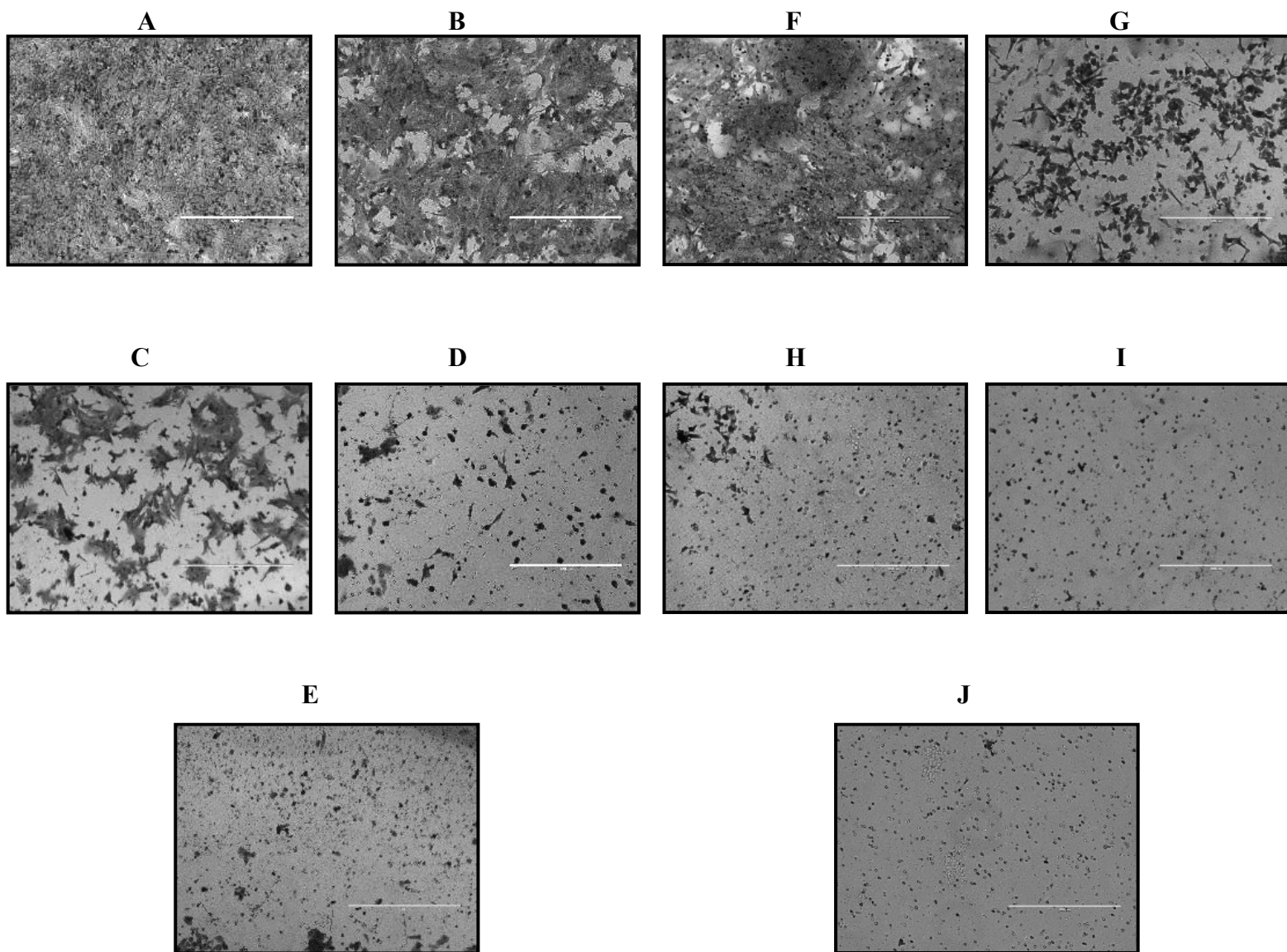


Figure 5: Representative images (10X magnification) of three replicate experiments of invasion using Boyden chambers in 4T1 and B16 cells after 24 hr treatment with CR-1-31-B.

(A) 4T1 cells control, (B) 4T1 cells 1 nM CR-1-31-B, (C) 4T1 cells 10 nM CR-1-31-B, (D) 4T1 cells 100 nM CR-1-31-B, (E) 4T1 cells 200 nM CR-1-31-B.

(F) B16 cells control, (G) B16 cells 1 nM CR-1-31-B, (H) B16 cells 10 nM CR-1-31-B, (I) B16 cells 100 nM CR-1-31-B, (J) B16 cells 200 nM CR-1-31-B.

N=3

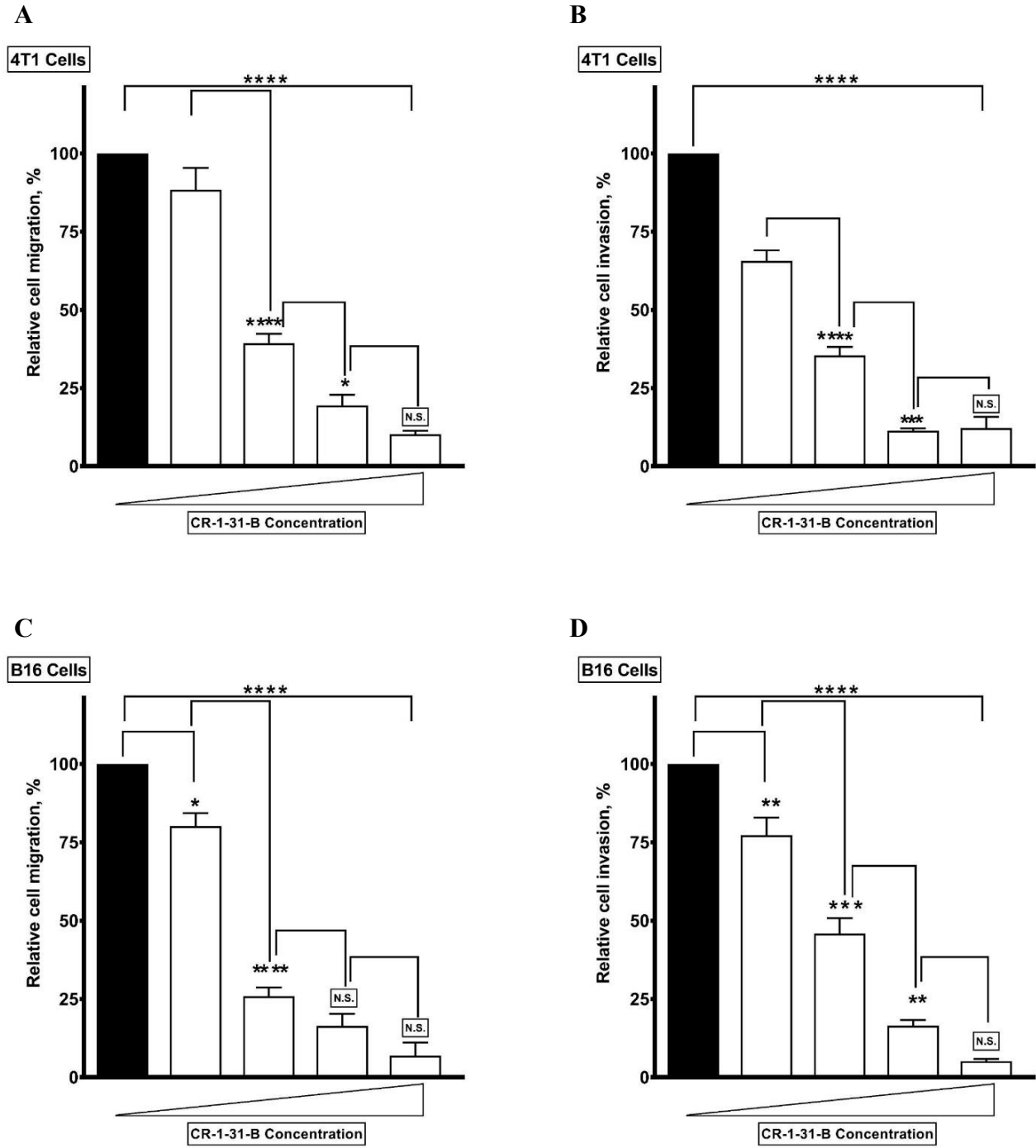


Figure 6: Quantification of Boyden chamber migration and invasion at 24 hr. Concentration-response (1-200 nM) or CR-1-31-B in 4T1 and B16 cells.

- (A) Migration of 4T1 cells treated with 1-200 nM of CR-1-31-B,
- (B) Invasion of 4T1 cells treated with 1-200 nM of CR-1-31-B,
- (C) Migration of B16 cells treated with 1-200 nM of CR-1-31-B,

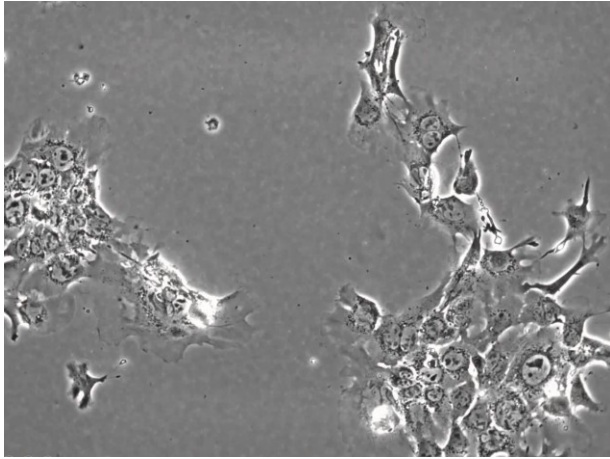
(D) Invasion of B16 cells treated with 1-200 nM of CR-1-31-B,
Data are mean \pm SEM (n = 3). *P < 0.05, **P < 0.01, ***P < 0.001, ****P < 0.0001; ns,
nonsignificant using 1-way ANOVA with Bonferroni Post-Hoc test.

3.5 Random migration is reduced upon CR-1-31-B treatment in TNBC cells

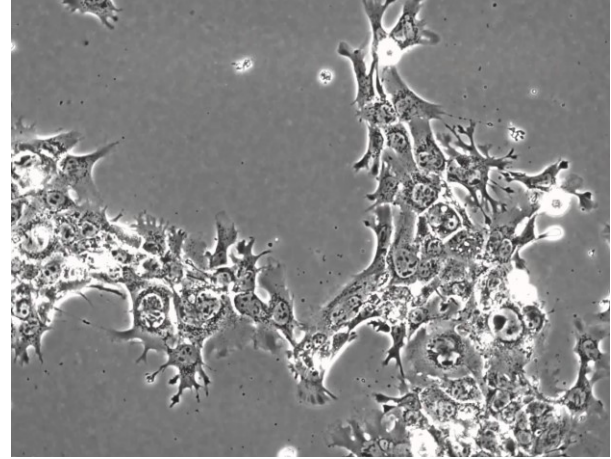
As previously mentioned, migration is a vital step in the process of cancer progression into metastasis. Many parameters of migration can be analyzed using time-lapse microscopy. These include random migration path, migration speed, and directional persistence. This technique allows for the visualization and analysis of single cell migration and can follow the movement and characteristics of particular cells over the course of an experimental analysis, [124], which in this case, was 24 hr.

Migration was significantly reduced with increasing concentrations of CR-1-31-B (1 – 200 nM) in TNBC cells (Figure 7). These are images taken at the beginning and end of the 24 hr treatment, and it should be noted that the movies corresponding to these images do a better job of visualizing the drastic changes in migration speed. Images are taken every 15 min over the 24 hr treatment period, and a movie is produced by taking all of the images and sequentially going through them at 10 frames/sec. As we saw in the Boyden chamber experiments, this reinforced that evidence, and points to CR-1-31-B as a potent agent against cancer cell migration.

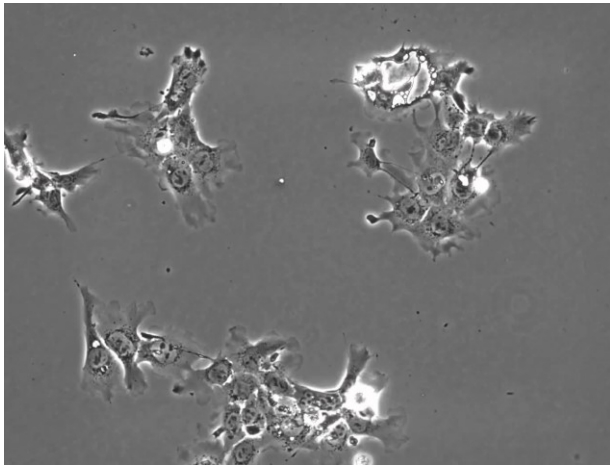
A



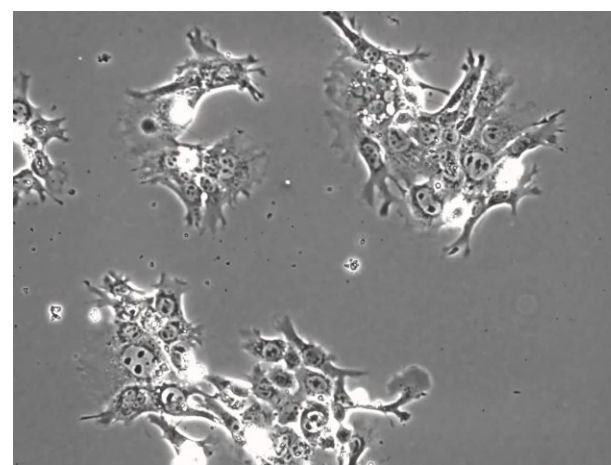
B



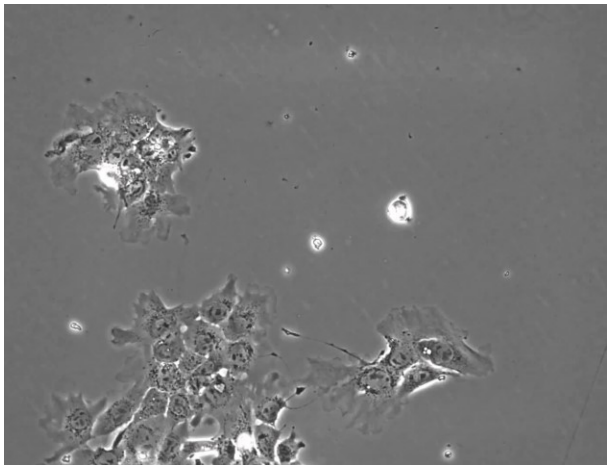
C



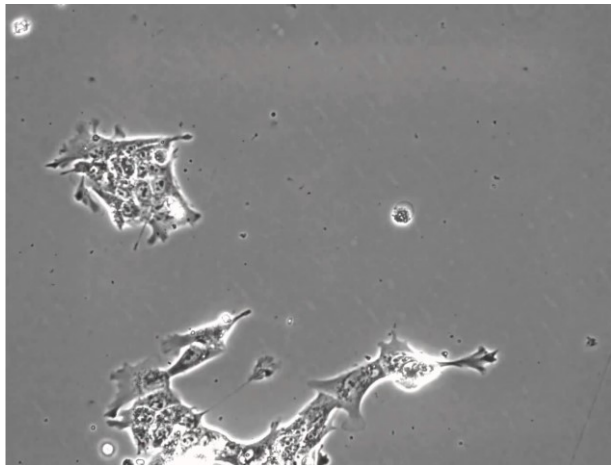
D



E



F



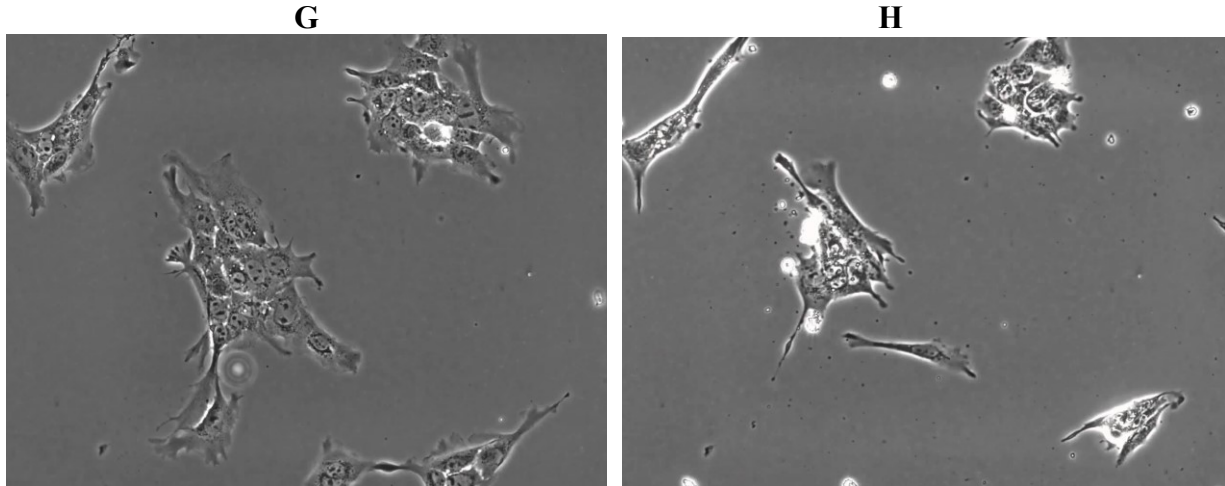


Figure 7: Representative images two replicate experiments of cellular migration of 4T1 cells treated with 1-200 nM or CR-1-31-B using time lapse microscopy. ‘Start’ corresponds to time = 0 hr, and ‘end’ corresponds to 24 hr after initiation of treatment (the corresponding movies demonstrate the change in migration speed more significantly).

(A) Control start, (B) Control end,
(C) 1nM start, (D) 1nM end,
(E) 10 nM start, (F) 10 nM end,
(G) 100 nM start, (H) 100 nM end
N=2

3.6 CR-1-31-B prevents collective cell migration in TNBC cells

We thoroughly tested the ability of these cells to migrate under various conditions, and as singular cells. In this set of experiments we wanted to assess the ability of cells to migrate collectively in real-time. Accordingly, we tested CR-1-31-B in 4T1 TNBC cells and found that as compared to DMSO treated control cells (Figure 8A and 8B), cells treated with only 1 nM CR-1-31-B showed a dramatic decrease in their ability to fill in the wound after 24 hours (Figure 8E and 8F). The main advantage of using specialized ImageLock 96-well plates is that it allows for precise recognition of the wound/scratch made by the Essen Wound maker. The Essen WoundMaker is a 96-pin mechanical device that is specifically tailored for these plates then creates a wound of 700-800 μm in thickness. After the wound is created, cells collectively migrate in order to fill in the gap/wound made by the WoundMaker.

The anti-tumor antibiotic mitomycin C was used some conditions. Mitomycin C interferes with enzymes in DNA replication, and is a well-known anti-proliferative agent. Treatment with mitomycin C was initiated 2 hr before CR-1-31-B treatment in order to prevent proliferation, and to thus give a much clearer representation of what CR-1-31-B does strictly in relation to anti-migratory behaviour. Mitomycin C was therefore used either in 4T1 cells alone (Figure 8C and 8D), or in conjunction with CR-1-31-B (Figure 8G and 8H) to help tease out the difference between simple inhibition of proliferation as compared to inhibition of migration due to CR-1-31-B treatment.

The data was quantified and graphed to show changes in migration after treatment with various concentrations of CR-1-31-B (1 -200 nM) on its own after 24 hr (Figure 9A), and in groups pre-treated for 2 hr with mitomycin C followed by the same 24 hr of CR-1-31-B

treatment (Figure 9B). As we saw with other *in vitro* assessments using this compound, we found a profound effect on wound closure, suggesting that this compound is also able to prevent collective cell migration.

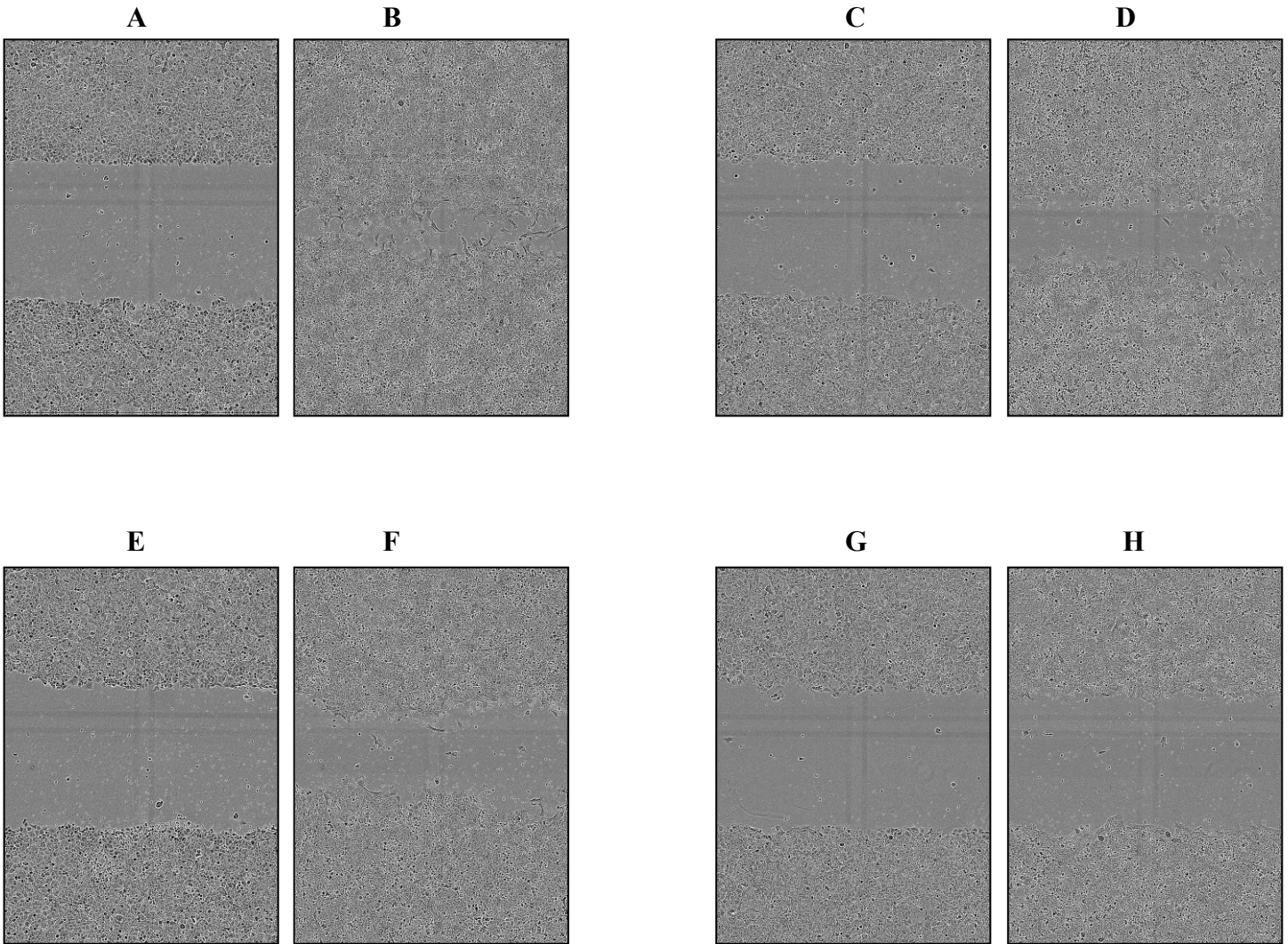
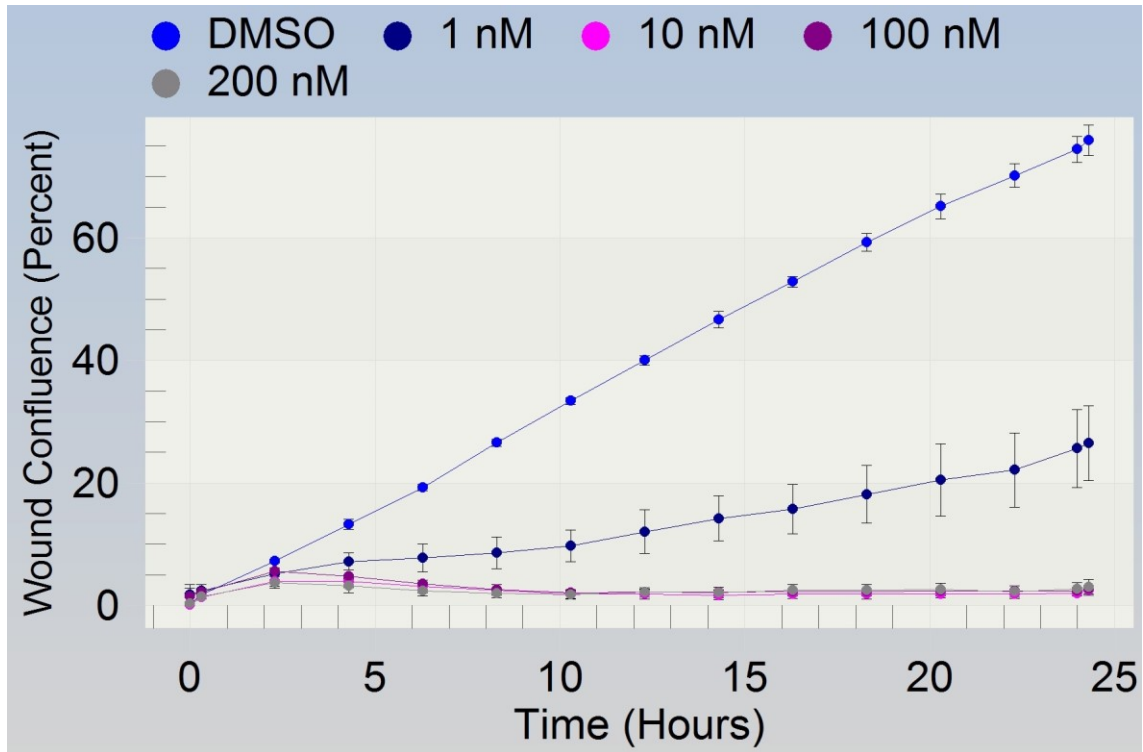


Figure 8: Representative images of two replicate experiments of wound confluence of 4T1 cells at 0 and 24 hr treated with 1 nM CR-1-31-B, with or without mitomycin C pre-treatment. **(A)** Control 0 hr, **(B)** Control 24 hr, **(C)** Mitomycin C alone, 0 hr, **(D)** Mitomycin C alone, 24 hr, **(E)** 1nM CR-1-31-B, 0 hr, **(F)** 1nM CR-1-31-B, 24 hr, **(G)** 1nM CR-1-31-B + mitomycin C, 0 hr **(H)** 1nM CR-1-31-B + Mitomycin c, 24 hr.

A



B

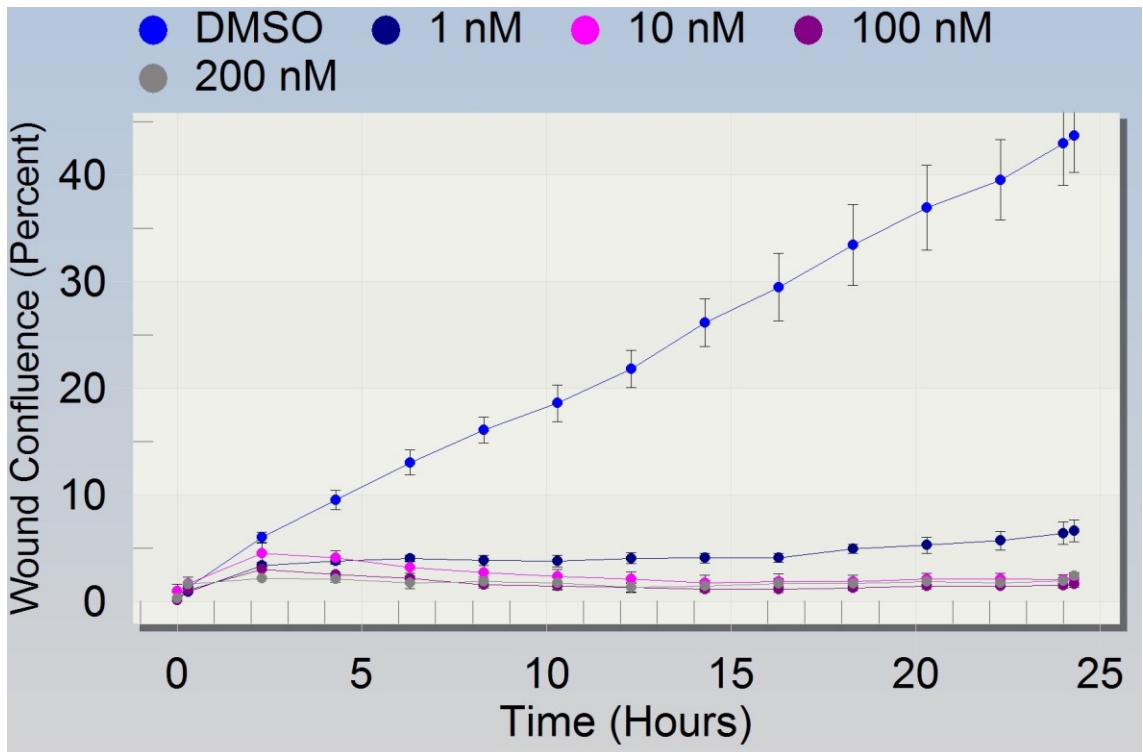


Figure 9: Quantification wound confluence of 4T1 cells over 24 hr period treated with 1-200 nM CR-1-31-B, with or without mitomycin C pre-treatment.

(A) CR-1-31-B concentration-response over 24 hr period, **(B)** CR-1-31-B + mitomycin C treatment concentration-response over 24 hr period.

N=2. Data are mean \pm SEM

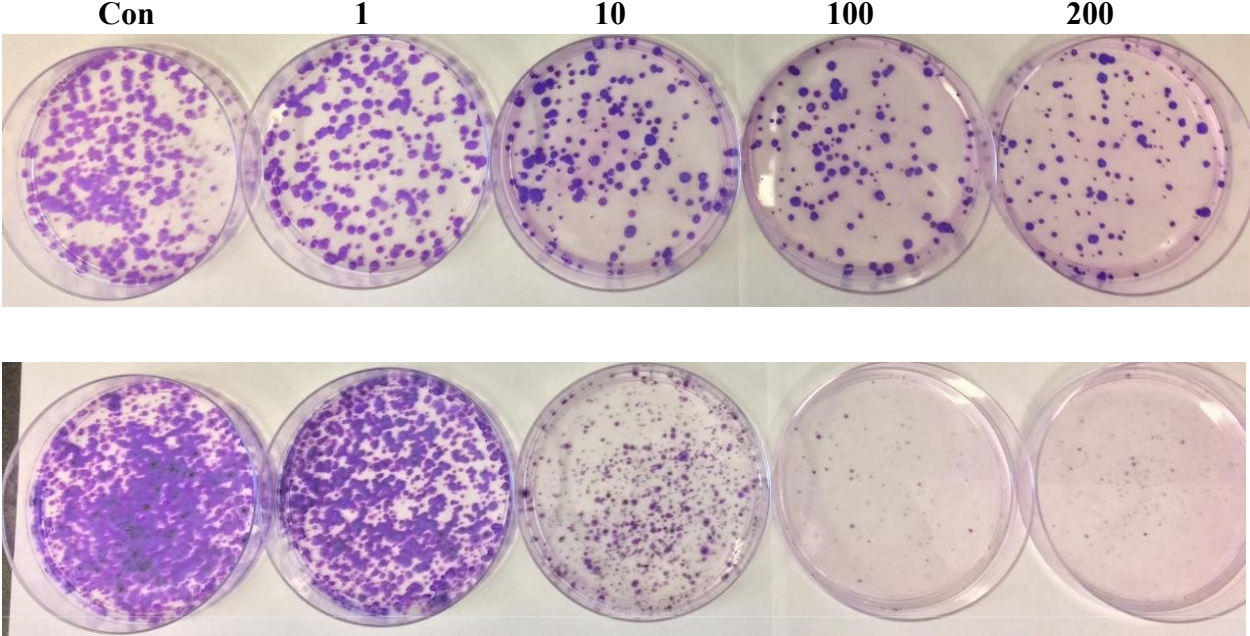
3.7 Treatment with CR-1-31-B reduces colony forming capabilities in TNBC cells

The colony formation assay (also sometimes referred to as a clonogenic assay), assess the capability that a single cell possess has to become into a colony, and can be used with essentially any cultured cells [41, 125]. A colony is typically defined as a group of 50 or more cells, and after initial seeding, the cells are given the ability to form into these colony for ~1-2 weeks. The intent is to replicate how stressful situations affect the ability of a cell to survive and to undergo “unlimited” division [41, 125]. The colony formation assay is an excellent tool to assess cytotoxic compounds, and gives an indication of metastasis [125]. We formed the colony formation assay by treated cells for 24 hours with varying concentrations of CR-1-31-B (1 - 200 nM), and then trypsinized, counted, and seeded 1000 cells from each treatment condition into a 10 cm plate. After one week cells are washed, fixed, and stained with crystal violet, colonies are counted. The representative images of 4T1 and B16 cells is seen in the top and bottom panels respectively (Figure 10A). Quantification for 4T1 (Figure 10B) and B16 cells was also performed (Figure 10C).

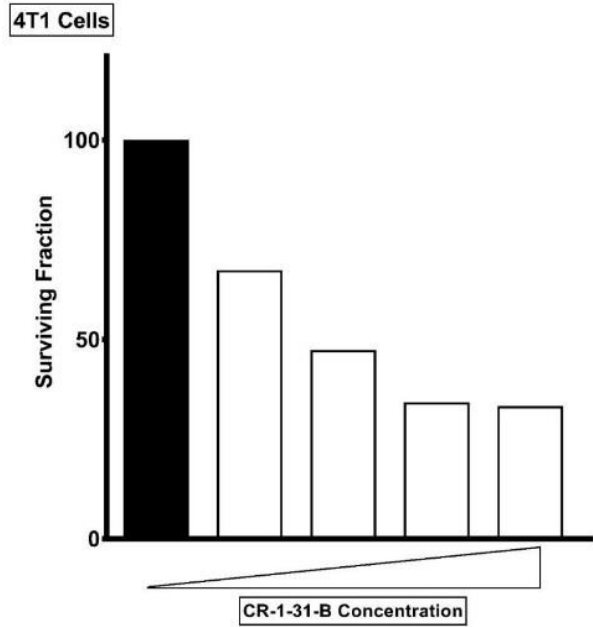
We also desired to see how a more long term treatment condition will affect these cells. We therefore decided to treat cells with 1nM and 10nM CR-1-31-B for 72 hr (media with drug replaced every 24 hr), followed by replating of cells as was done before. Representative images of 4T1 and B16 cells is seen in the top and bottom panels respectively (Figure 11A). Quantification for 4T1 (Figure 11B) and B16 cells was also performed (Figure 11C). This was another clear indication to use that this compound is not simply acting in an anti-proliferative or cytotoxic manner, since each 10 cm plate started out with 1000 cells from each condition. It is

instead suggests that in both cells types, treatment with CR-1-31-B induces profound changes leading to a drastic decrease in colony forming capability.

A



B



C

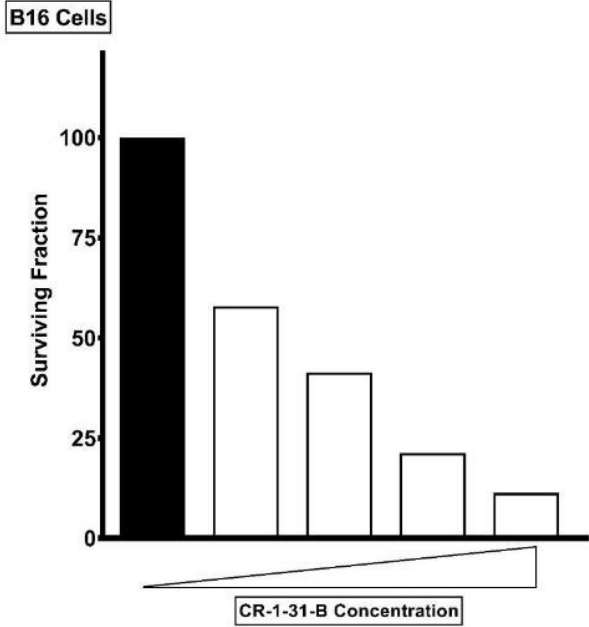
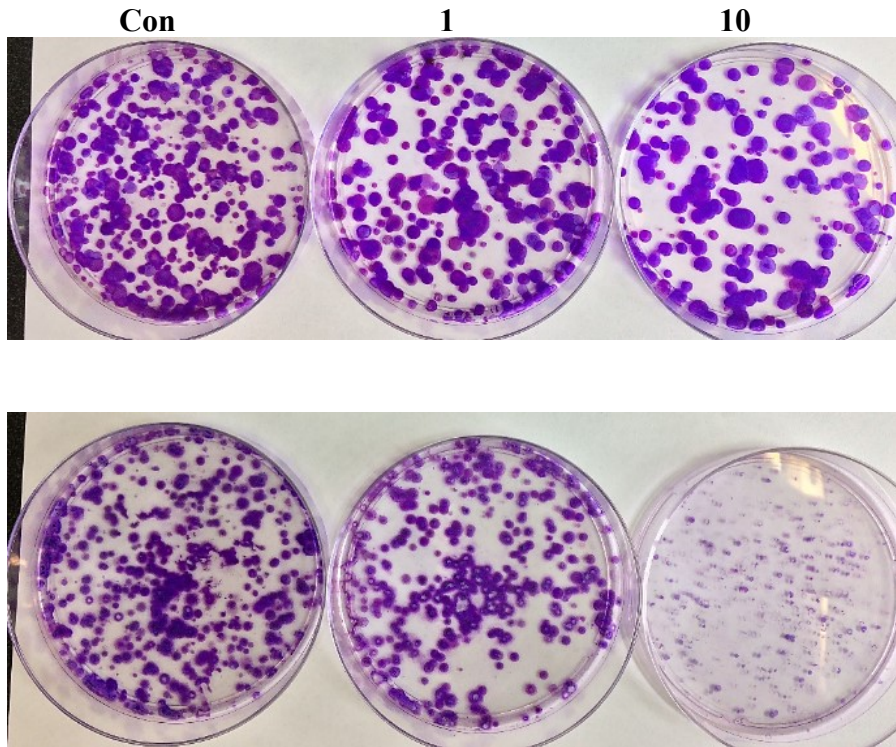
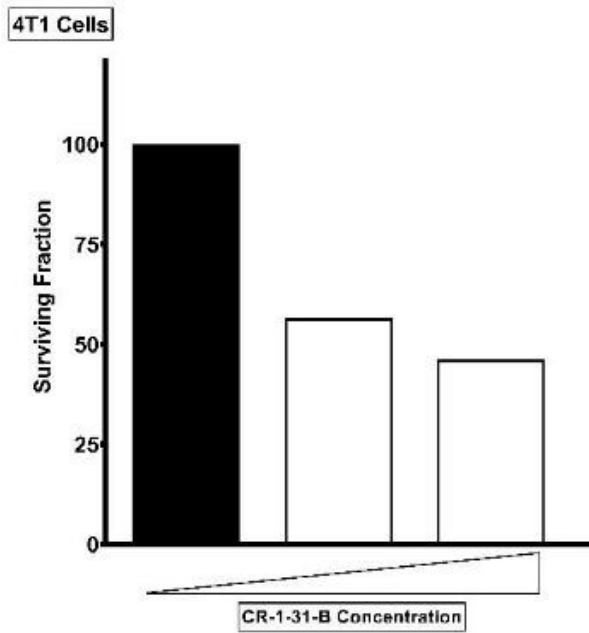


Figure 10: Representative images of two replicate experiments and quantification of colony formation in 4T1 and B16 cells following 24 hr of pre-treatment with CR-1-31-B (1-200 nM).
(A) Representative images of colony formation of 4T1 cells (top panel), and representative images of B16 cells (bottom panel),
(B) Quantification of colony formation of 4T1 cells,
(C) Quantification of colony formation of B16 cells.
N=2

A



B



C

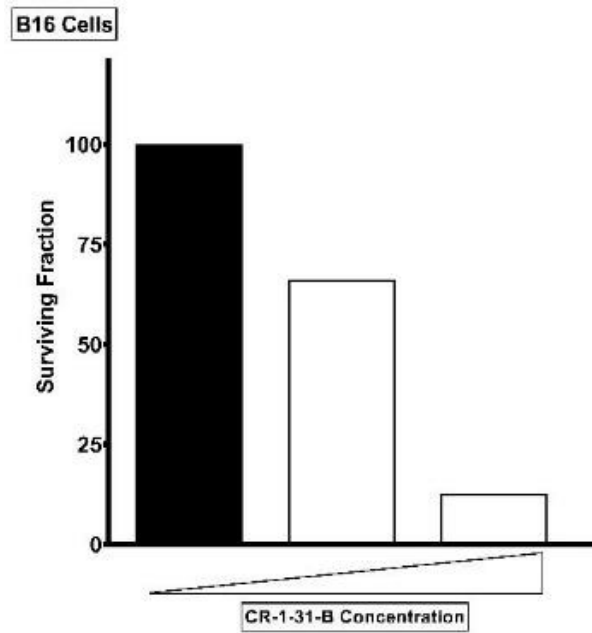


Figure 11: Representative images of two replicate experiments and quantification of colony formation in 4T1 and B16 cells following 72 hr of pre-treatment with CR-1-31-B (1 and 10 nM).
(A) Representative images of colony formation of 4T1 cells (top panel), and representative images of B16 cells (bottom panel)
(B) Quantification of colony formation of 4T1 cells,
(C) Quantification of colony formation of B16 cells.
N=2

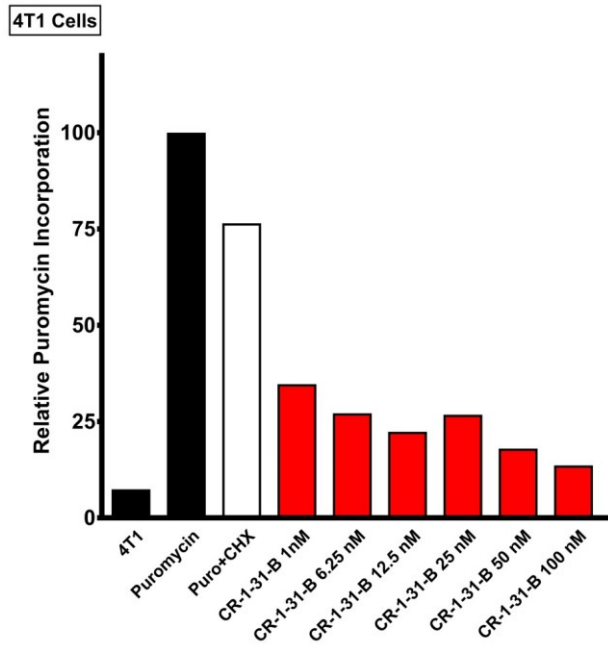
3.8 CR-1-31-B treatment downregulates the rate of protein synthesis *in vitro* and *in vivo*

Our lab has previously utilized the non-radioactive puromycin-labelling assay, also referred to as (SUnSET) [126]. As delineated in the original 2009 publication it is an assay used to assess the rate of protein synthesis [127]. Puromycin is added directly to the culture media shortly before collection of cells. We also utilized cycloheximide as a positive control, as it is a known protein synthesis inhibitor. The cells are then collected on ice, and the cellular extracts are prepared for western blotting, followed by probing with anti-puromycin. 4T1 cells appear to display a concentration-dependent decrease in protein synthesis with corresponding increases in CR-1-31-B concentration (Figure 12A). β -actin was used as a loading control, and showed no difference between groups (Figure 12B). The Ponceau S stained gel is shown in Figure 12C. Quantification of the signal (used in Figure 12A) was achieved by subtracting the unlabelled protein control from the total signal in each lane seen in Figure 12D.

We also wanted to see if CR-1-31-B injection in BALB/c mice is directly inhibiting protein synthesis. As was shown using 4T1 cells, this experiment serves as an excellent positive control to help deduce if this compound is indeed inhibiting protein synthesis. As was done in experiments utilizing 4T1 cells as a tumor model to assess the efficacy of CR-1-31-B treatment (see below), we wanted to directly measure if this compound reduces global protein synthesis. Once 4T1 tumors were palpable in BALB/c mice, they were injected IP with CR-1-31-B (0.2mg/kg) for one hour before harvesting of livers. We then performed a similar experiment as was done with the 4T1 cells *in vitro*. We found that treatment with CR-1-31-B led to a decrease in the overall rate of protein synthesis in these mouse livers (Figure 13A). Our loading control β -

actin show no difference between groups (Figure 13B). The Ponceau S stained gel is shown in Figure 13C. Quantification of the signal was achieved by subtracting the unlabelled protein control from the total signal in each lane (Figure 13D). These experiments demonstrate that CR-1-31-B is directly reducing the rate of protein synthesis both *in vitro* and *in vivo*, which helps to validate our use of this compound to try and reduce primary tumor burden (see below)

A

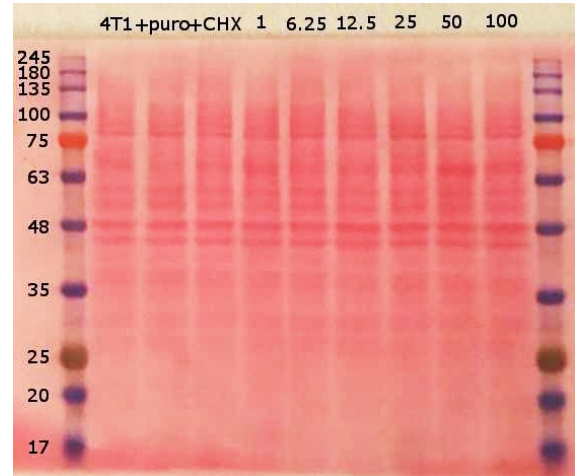


B



C

Ponceau S stained gel



D

Full membrane

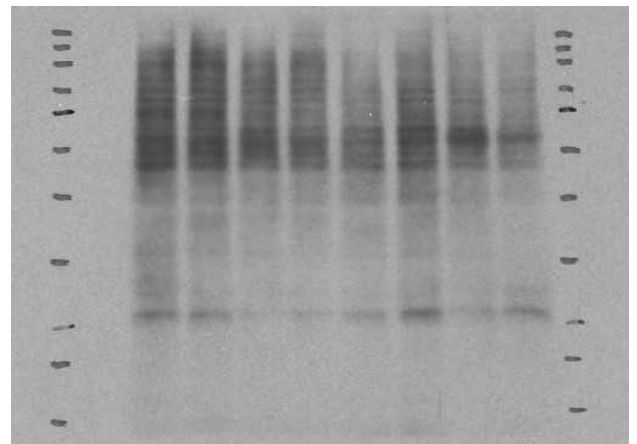


Figure 12: SUnSET assay in 4T1 cells treated with CR-1-31-B (1-100 nM)

Representative images and quantification of one replicate experiment

(A) Changes in protein synthesis in 4T1 cells treated with CR-1-31-B (puromycin incorporation).

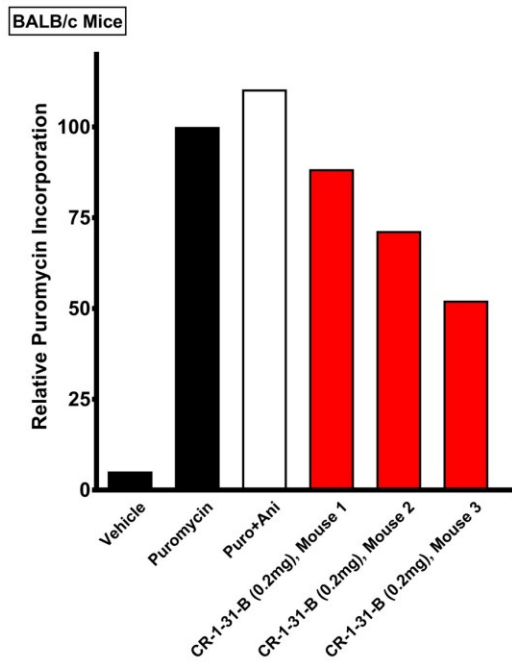
(B) β -actin loading control western blot

(C) Ponceau S stained gel

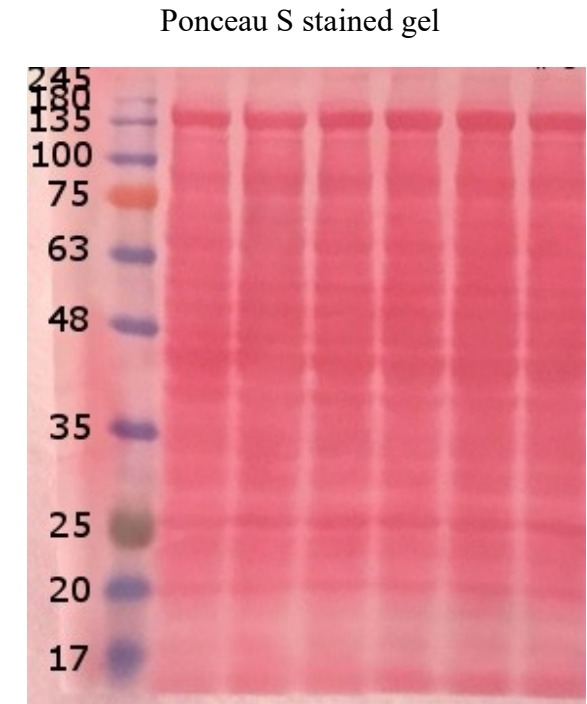
(D) Full membrane used for western blot quantification in these experiments

N=1

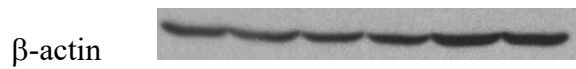
A



C



B



D

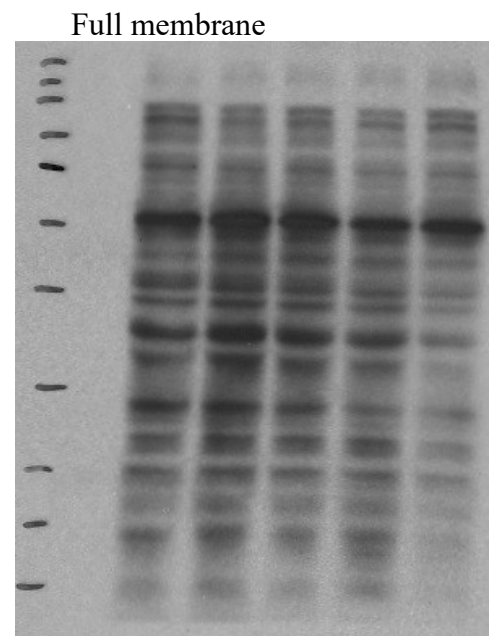


Figure 13: SUnSET assay in livers from BALB/c mice treated with CR-1-31-B (1-100 nM)

(A) Changes in protein synthesis in mouse livers treated with CR-1-31-B (puromycin incorporation).

(B) β -actin loading control western blot

(C) Ponceau S stained gel

(D) Full membrane used for western blot quantification in these experiments

N=1

3.9 CR-1-31-B treatment reduces tumor burden in NOG mice

Given the robust results we found with all of the various *in vitro* assessments were performed looking at the role of CR-1-31-B in TNBC cells we wanted to look at its function in a more physiological model. Our first objective was to test the effect of this compound in severely immuno-compromised NOG mice. These mice display a severely compromised immune system since they lack NK cells, T cells, and B cells [128]. The timeline of the exact experimental protocol, and endpoints and assessments we did is shown below (Figure 14).

100,000 4T1-luc cells were orthotopically injected into NOG mice. Once tumors had grown to a palpable size, daily injections of CR-1-31-B (0.2mg/kg) for 14 days were initiated. This treatment led to a striking decrease in primary tumor burden (Figure 15A). We failed to observe any overt metastasis in compound treated mice. On the other hand, as one would expect, we did find some metastatic nodules (black circles) in the lungs of vehicle treated mice (Figure 15B). There difference in primary tumor size was very apparent and could be observed by eye, comparing the vehicle treated mouse in the top panel, to the CR-1-31-B treated mouse in the bottom panel (Figure 15C). In accordance with the caliper measurements and visual inspection in Figure 15A and 15C, we found a significant decrease in the tumor weight of mice treated with CR-1-31-B as compared to vehicle treated mice (Figure 15D). Significant signs of toxicity were not present as there was no difference in the weight of mice during the duration of the study (Figure 15E). Similarly, we found that the liver weight was the same between groups (Figure 15F). We did however find that the mice treated with CR-1-31-B did have significantly smaller spleen mass. These results provide strong evidence that CR-1-31-B is an effective treatment against TNBC in immuno-compromised mice.

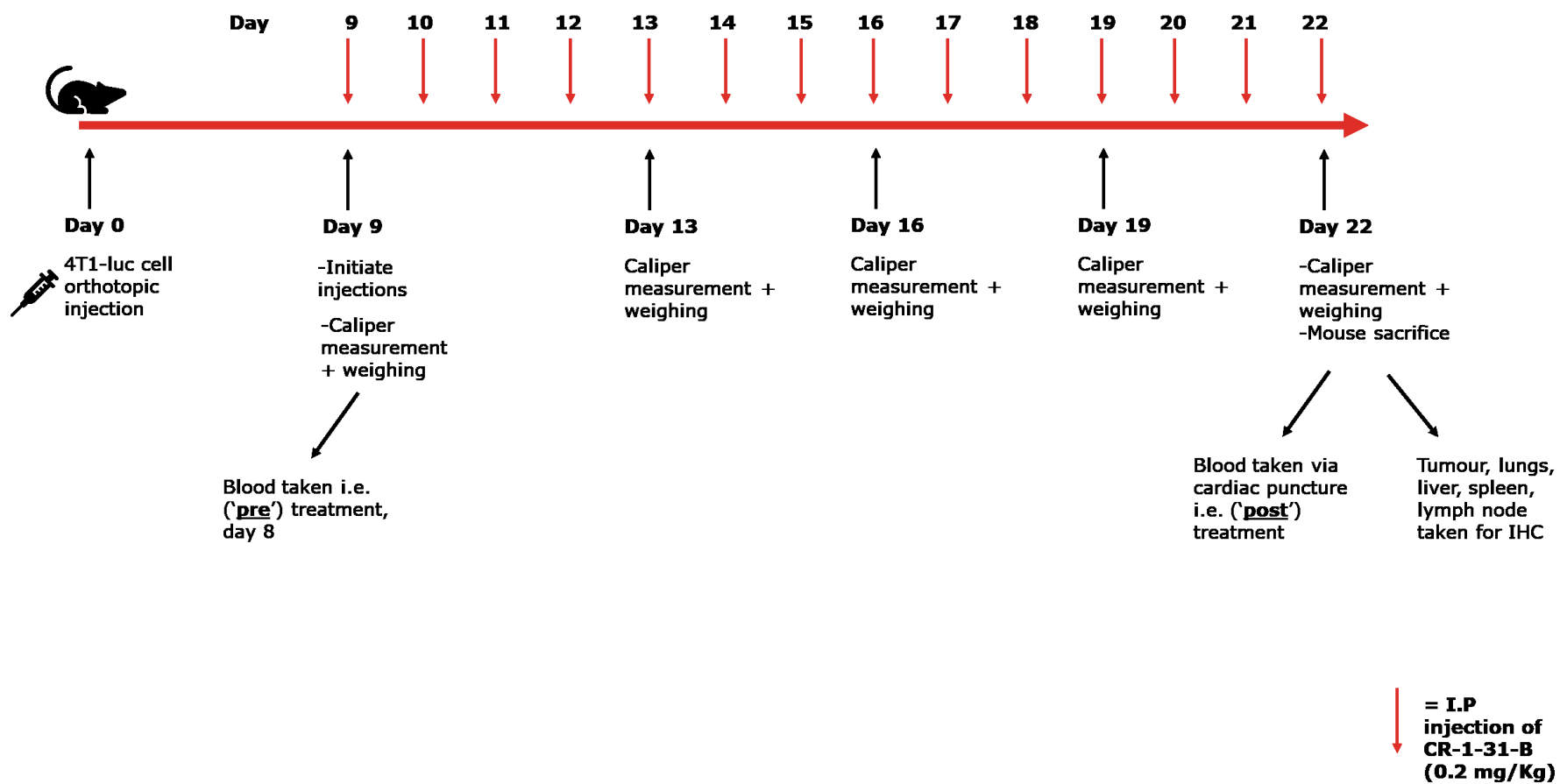


Figure 14: Timeline of Experimental Protocol (NOG Mice)

NOG mice were injected with 4T1-luc cells on day 0. After 9 days, caliper measurement and weighing was initiated. Caliper measurements and mouse weights were then taken every three days for the duration of the experiment. Starting from day 9, daily injections of CR-1-31-B (0.2 mg/kg) were initiated for the following 14 days. On day 22 mice were caliper measured, weighed, and sacrificed with their tissues being taken for IHC analysis.

N=5 per group

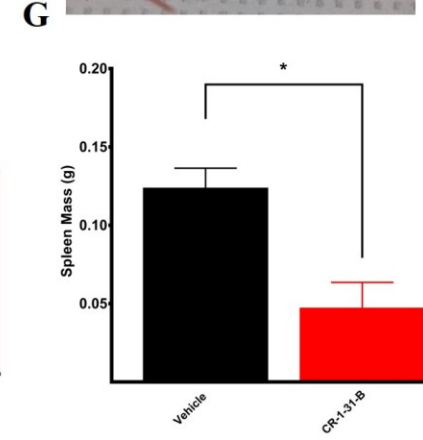
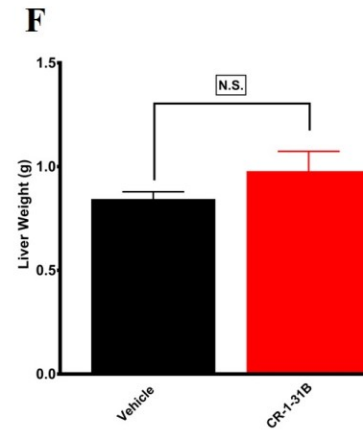
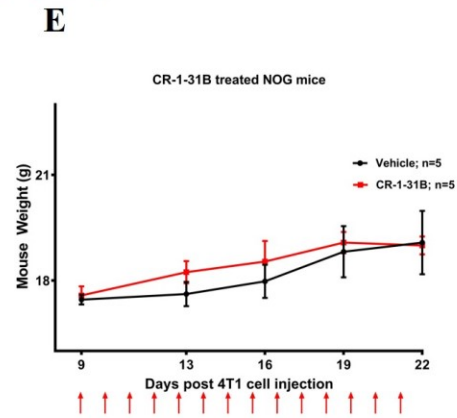
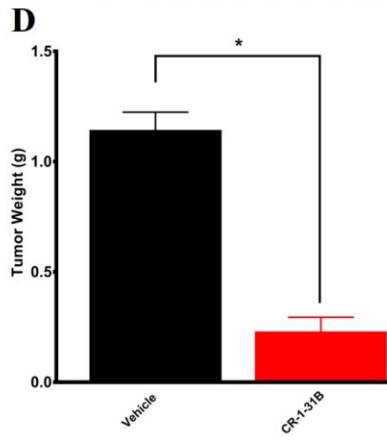
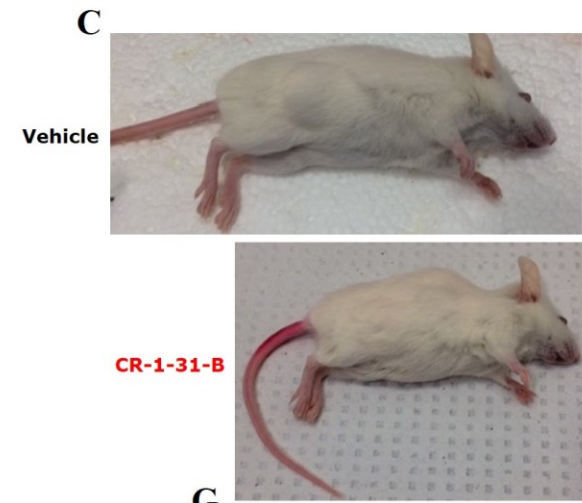
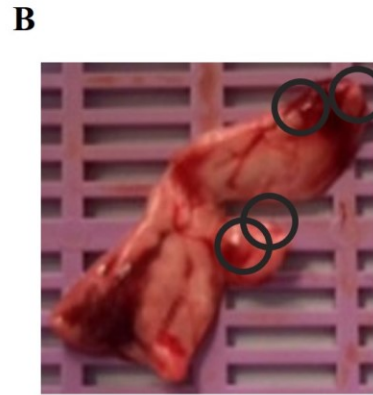
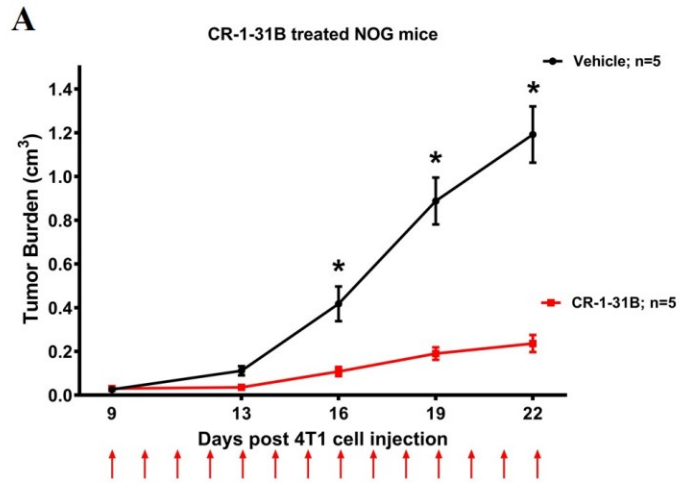


Figure 15: 14 days of CR-1-31-B treatment leads to striking reduction of primary tumor burden in NOG mice

(A) Primary tumor burden in vehicle and CR-1-31-B treated NOG mice (N=5)

(B) Representative image of 5 replicate animals showing overt lung metastasis

(C) Upper panel is a representative image of 5 replicate animals that were vehicle treated. Upper panel is a representative image of 5 replicate animals that were treated with CR-1-31-B

(D) Primary tumor weight in vehicle and CR-1-31-B treated NOG mice (N=5)

(E) Mouse weight (in grams) vehicle and CR-1-31-B treated NOG mice (N=5)

(F) Liver weight (in grams) vehicle and CR-1-31-B treated NOG mice (N=5)

(G) Spleen mass (in grams) vehicle and CR-1-31-B treated NOG mice (N=5)

Data are mean \pm SEM (N = 5). *P < 0.05, ns, nonsignificant using Student's T-test for tumor weight, liver weight, and spleen mass, and a 2-way ANOVA with Bonferroni Post-Hoc test for caliper measurements of tumor burden.

3.10 CR-1-31-B *increases* primary tumor burden in BALB/c mice

The next and perhaps most important series of experiments was to assess the role of eIF4A inhibition (with CR-1-31-B) in a syngeneic 4T1 TNBC model. The timeline of the exact experimental protocol, and endpoints and assessments we performed is outlined below (Figure 16).

Therefore, we used 4T1-luc cells, and injected 100,000 cells into syngeneic BALB/c mice. Once tumors were palpable, we treated mice with CR-1-31-B (0.2mg/kg) for 14 consecutive days. To our surprise, we found that tumor burden was actually increased in mice treated with CR-1-31-B as compared to vehicle treated mice (Figure 17A). Accordingly, the weight of the actual tumor from CR-1-31-B was significantly larger than the counterpart tumor from vehicle treated mice (Figure 17B). Spleen mass was also significantly larger in mice treated with CR-1-31-B (Figure 17C). Finally, although it was not statistically significant, there appears to be a trend for a decrease in overall mouse weight in mice treated with CR-1-31-B as opposed to vehicle treated mice (Figure 17D). This provides a very interesting juxtaposition, whereby eIF4A inhibition produces desirable effects in immuno-compromised mice (i.e. decrease in tumor burden), but is ineffective, and actual detrimental in a syngeneic immuno-competent setting.

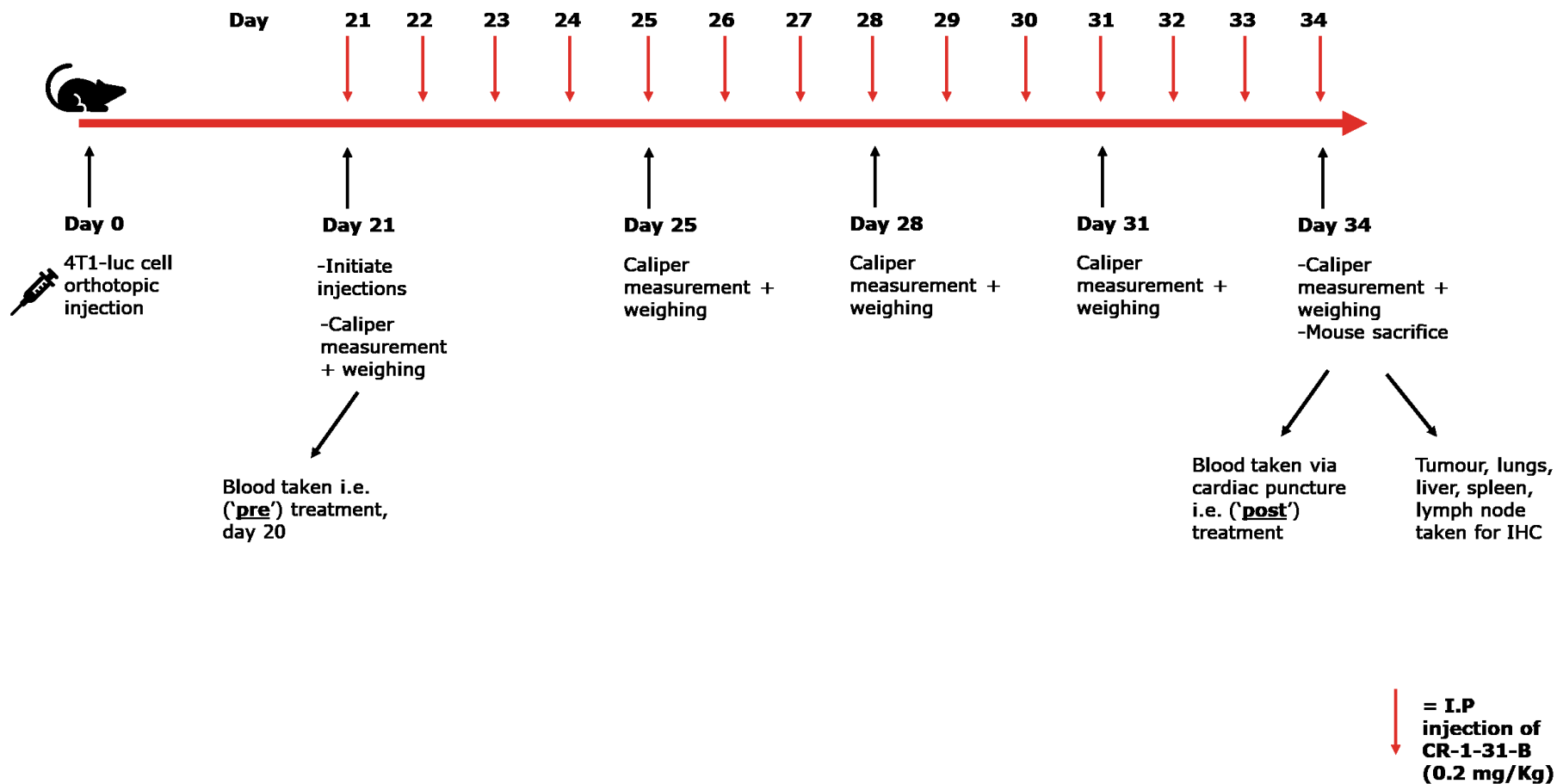


Figure 16: Timeline of Experimental Protocol (BALB/c Mice)

BALB/c mice were injected with 4T1-luc cells on day 0. After 21 days, caliper measurement and weighing was initiated. Caliper measurements and mouse weights were then taken every three days for the duration of the experiment. Starting from day 21, daily injections of CR-1-31-B (0.2 mg/kg) were initiated for the following 14 days. On day 34 mice were caliper measured, weighed, and sacrificed with their tissues being taken for IHC analysis.

N=9 per group

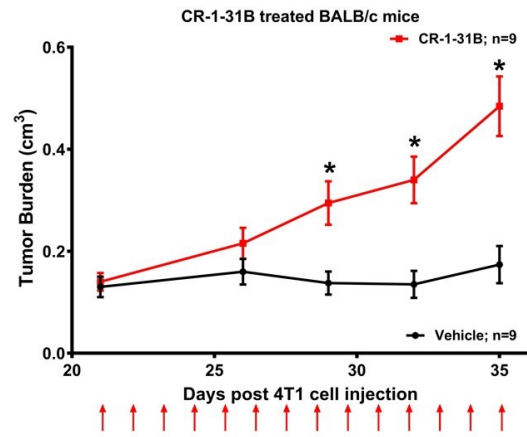
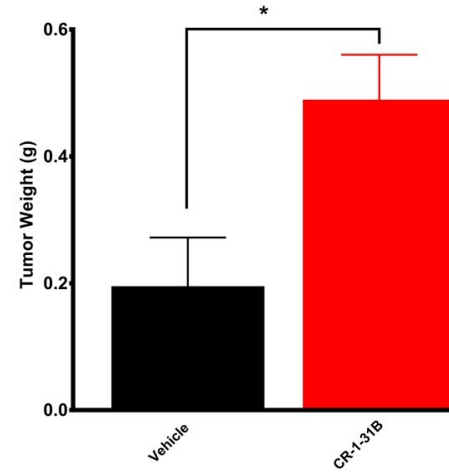
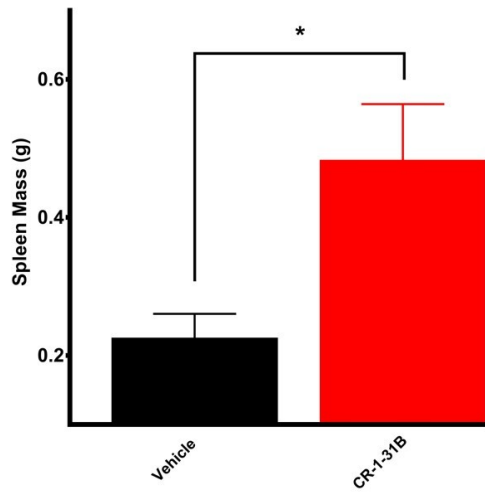
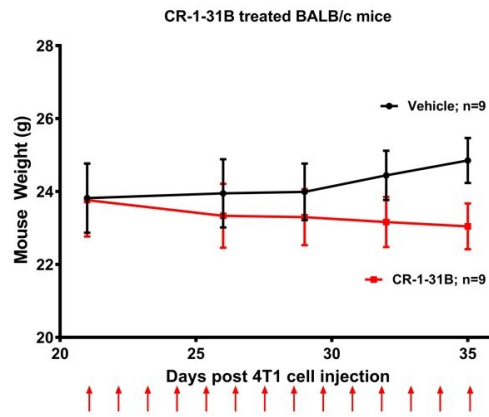
A**B****C****D**

Figure 17: 14 days of CR-1-31-B increase primary tumor burden in BALB/c mice

(A) Primary tumor burden in vehicle and CR-1-31-B treated BALB/c mice (N=9)

(B) Primary tumor weight in vehicle and CR-1-31-B treated BALB/c mice (N=9)

(C) Spleen mass in vehicle and CR-1-31-B treated BALB/c mice (N=9)

(D) Mouse weight (in grams) in vehicle and CR-1-31-B treated BALB/c mice (N=9)

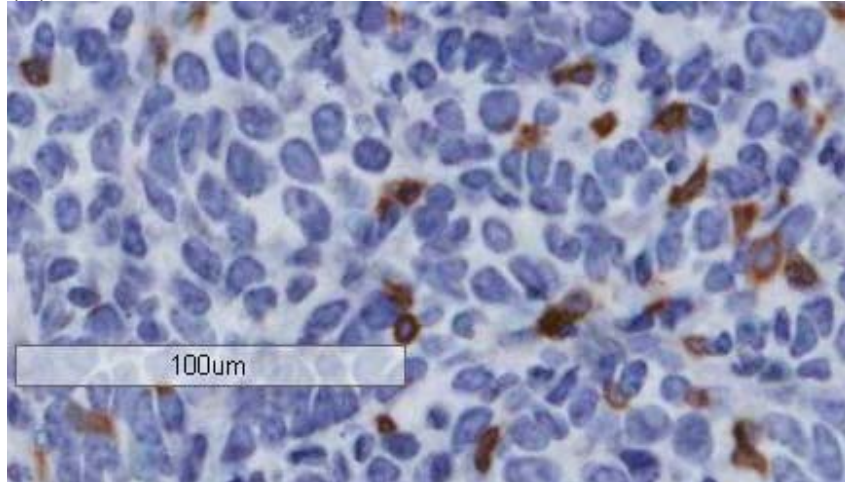
Data are mean \pm SEM (N = 9). *P < 0.05, Student's T-test for tumor weight and spleen mass, and a 2-way ANOVA with Bonferroni Post-Hoc test for caliper measurements of tumor burden.

3.11 BALB/c mice treated with CR-1-31-B have less tumor T cell infiltration

Given the discrepancy in the results we found in our two *in vivo* models (BALB/c and NOG), we were very interested in assessing the role that CR-1-31-B has in the TME. We decided to do IHC to look at T cell infiltration, and found that in BALB/c mice, treated with CR-1-31-B led to a large reduction in the amount of T cells infiltrating into the tumor (Figure 18B). This strongly implicates the immune system as a direct target of CR-1-31-B therapy. It is also interesting to note that this lack of T cell infiltration into a tumor could be a hindrance for adequate efficacy with PD-L1 immune checkpoint blockade [129]. This is important, given that PD-L1 therapy is emerging as a very interesting and powerful form of treatment in cancer, but suggests that it may not work in conjunction with an eIF4A inhibitor such as CR-1-31-B.

In summary, our results suggest that inhibition of eIF4A with CR-1-31-B is a viable treatment strategy in mice that lack a functional immune system, but appears to not be a good treatment as a monotherapy in immuno-competent BALB/c mice. This discrepancy in results and potential mechanism(s) of action is summarized in Figure 19.

(A) Vehicle



(B) CR-1-31-B

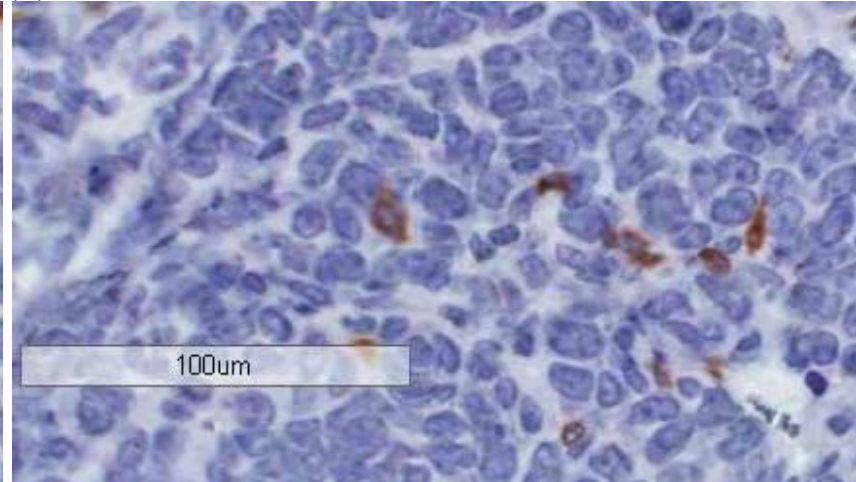


Figure 18: T cell infiltration in tumors from BALB/c mice as detected by immunohistochemistry with anti-CD3

(A) T cell infiltration from vehicle treated BALB/c mice (N=9)

(B) T cell infiltration from CR-1-31-B treated BALB/c mice (N=9)

These are representative IHC images of nine replicate experiments.

N=9

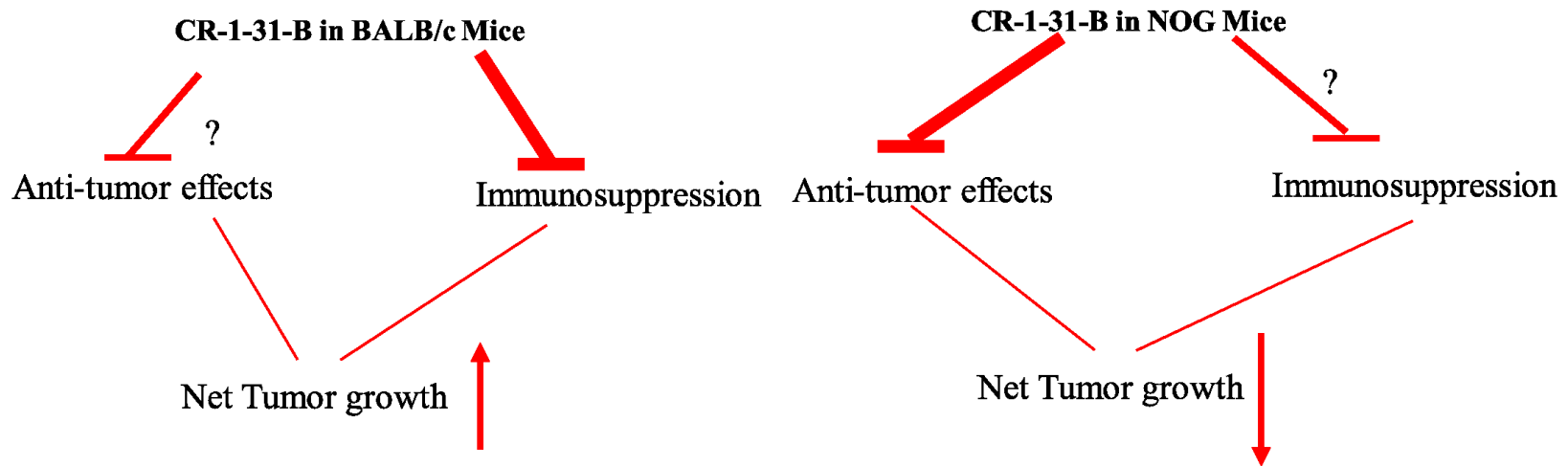


Figure 19: Current understanding of data

This figure represents our current understanding of the data. It suggests that CR-1-31-B is most likely having a direct anti-tumor effect in NOG mice. However, in BALB/c mice any direct anti-tumor effect that may be occurring appears to be significantly offset by an apparent downregulation of some as to be fully elucidated immune components. We thus end up with a dichotomy whereby we see a net tumor reduction in NOG mice, but a significant net tumor growth in BALB/c mice

DISCUSSION

For the experiments shown in this thesis, we employed the use of a synthetic derivative of silvestrol, given that its simpler chemical structure allows greater ease of synthesis, and its enhanced bioavailability, as previously shown [130]. The use of a 4T1 syngeneic system was chosen as it is an excellent animal model representation stage IV human breast cancer. Dozens of compounds have been tested *in vitro* and murine models for their anti-cancer effects in a translationally-mediated manner, but as mentioned, the ‘translation’ of these results into the clinic leaves much to be desired [54]. The research presented here provides new and exciting discoveries in regard to the role of translational inhibition in the TME. This work is original as it points to previously underappreciated roles of eIF4A inhibition in a syngeneic immuno-competent setting. The most important discovery stemming from this work points to the lack of efficacy of eIF4A inhibition in an immuno-competent setting. Not only lack of efficacy, but we actually found that burden was significantly exacerbated in BALB/c mice when treated with the eIF4A inhibitor CR-1-3-1B. The current thesis supports the notion that small molecule inhibitors of translation such as CR-1-3-1B, can display cytotoxicity towards established breast cancer tumors, but in immunocompetent settings appear to also have toxicity toward certain immune populations. This is original and significant work moving potentially the entire field of translation forward, given that previous studies failed to address the role of eIF4A inhibition in this important setting.

As previously mentioned, deregulated mRNA translation can lead to therapeutic resistance. The eIF4F complex is thus a tantalizing target for cancer therapy, and has been referred to as a ‘nexus’ of resistance and cancer development [53, 131]. The Sonenberg lab has

been interested in detailing the effect of eIF4F inhibition, given its role in encoding proteins that are important in cellular survival, such as cyclins and MCL1 [132]. In particular, it has also been shown that specific mRNAs are sensitive to changes in eIF4A, including those intimately linked to cancer such as TGF- β 1, and transcription factors such as NOTCH1 and c-myc, which is mediated at least in part by the complexity of their 5' UTRs [60, 85]. In addition, drug resistance can occur when targeting upstream pathway components such as PI3K/mTOR, since amplified eIF4E can prevent successful use of these inhibition [133]. Interestingly, in the same study, MYC amplification also caused resistance to drug inhibition [133]. This suggests that targeting eIF4A with drugs such as silvestrol which is known to downregulate MYC, could be a viable strategy, at least in certain models. Indeed, silvestrol has been shown to possess the ability to effectively inhibit translation of MYC in murine colorectal cancer [134]. It is interesting to note that not all eIF4A, and not even all flavaglines are created equal. RiboSeq data demonstrated that 5' UTR structure did not play a major role in rocaglamide A effectiveness, and that this compound caused eIF4A to attach onto polypurine sequences [135]. Relevant to our experiments, it is known that upon its binding to mRNA, silvestrol, and synthetic derivatives such as CR-1-31-B reversibly sequester eIF4A away from its binding partners [94].

When compared to eIF4E, there has been a noticeable lack of studies addressing the role of eIF4A in tumorigenesis. However, this is strong evidence to suggest that targeting eIF4A is a viable and logical target. In particular, a recent study demonstrated that tissue microarray from thousands of patients pinpointed eIF4A expression as a statistically significant independent prognostic indicator of ER-negative breast cancer [60]. This link is supported by previously published pre-clinical data demonstrated that inhibition of eIF4A with silvestrol leads to a

significant decrease in primary tumor burden, and induction of apoptosis in a breast cancer model [61].

Taking a big picture look at the work presented here, we have found that the host is critical to the end result of eIF4A inhibition. This was clearly demonstrated in our mouse models, whereby eIF4A inhibition using CR-1-31-B led to anti-cancer effects against primary tumor burden in immuno-compromised mice (hosts). However, there was a very clear juxtaposition, and pro-tumorigenic effects observed in immuno-competent BALB/c mice, prompting us to reformulate our original hypothesis to our current one, where we believe that this compound is inhibiting the adaptive immune response toward tumors established by 4T1 cells, and this inhibition is so robust that it is in essence counteracting any potential anti-tumor effects of this compound being observed in this setting.

Future experimental work should focus on assessing the role of eIF4A inhibition in a variety of systems. This is an important point given that aforementioned work has shown that eIF4E and eIF4A target different sets of transcripts based on features in the 5' UTR. Thus, previous studies linking eIF4E to various cancers would not necessarily carry over to inhibition of eIF4A, and vice versa. This suggests that certain anti-cancer effects may be eIF4F subunit-specific [56]. Continued focus on elucidating the role of eIF4A inhibition in breast cancer, and melanoma is paramount, particularly in an immuno-competent setting. It may be tempting to make sweeping generalized statements regarding flavaglines, but it may be the case that multiple flavaglines need to be utilized in the same system to test for differences and similarities in effect toward established tumors. In addition, in order to exclude for cell-specific effects, it may be a good idea to test the role of inhibitors such as CR-1-31-B in immune-competent mice with tumors different from those caused by 4T1 cells. Thus, based on our current understanding, the

major concern of using silvestrol derivations is the possibility that they are not appropriate to be used in immuno-competent BALB/c mice, particularly using 4T1 cells as a model.

One potential avenue for future research could be to expand on the research presented here utilizing time lapse microscopy to look at changes in cellular migration after treatment with CR-1-31-B. Additional analysis on changes in this migration potential can take the form of looking at the speed at which cells are moving – this is done by manually monitoring the cell tracks of individual cells [101, 136]. Another interesting aspect of migration that can be analyzed using technology such as time lapse microscopy is directional persistence. This is typically quantified as a ratio of net displacement against total migration distance [137]. With respect to the data presented here, we would expect the cells to have a decreased ability in maintaining their path of movement. In addition, given our IHC results showing that T cell infiltration is hindered in BALB/c mice treated with CR-1-31-B, this deserves a more in-depth analysis. This result is not completely surprising, as previous work demonstrated that decreasing eIF4E has direct effect on T regulatory (Treg) development [72]. Thus, looking more specifically at how translation inhibitors, with a particular focus on eIF4A inhibitor molecules in a T cell biology setting is an exciting area of future investigation.

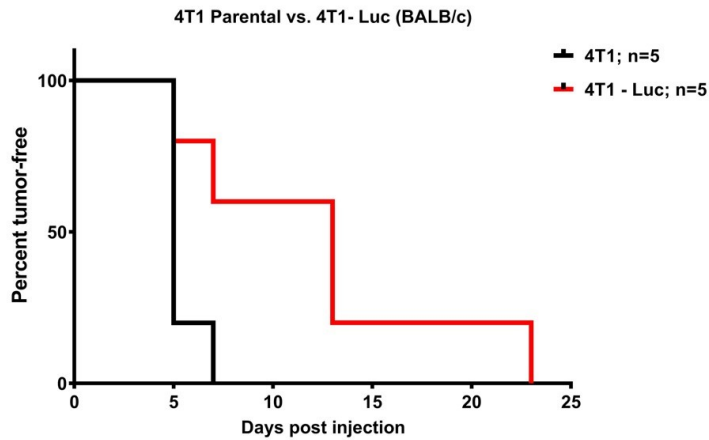
Additional relevant research on this project should also assess the specific and broad-ranging role of immuno-suppression in response to this inhibitor with the use of mass cytometry work, which is currently being developed and perfected in-house at the Goodman Cancer Centre. This will be done using a Helios mass cytometry, and will allow for robust analysis of various tumor sections to pinpoint which immune cells are being influenced by eIF4A inhibition, thereby allowing for the survival of 4T1 tumors in BALB/c (and can also be extended to other models such as B16). This work could look at a large range of infiltrating immune cells such as T cells

(both T effect and T regulatory), as well as neutrophils and macrophages. Mass cytometry is quickly emerging as a useful and powerful tool, as it can facilitate the simultaneous analysis of ~40 markers utilizing commonly used tissue sections. This will help derive information of cellular location and number within that tissue.

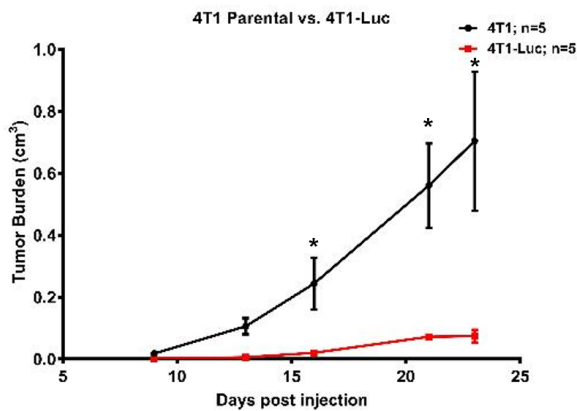
I believe that this thesis provides through *in vitro* characterization, and robust *in vivo* data to demonstrate the limitations and ineffectiveness of a specific eIF4A inhibitor (CR-1-31-B), and potentially others, in modulating an anti-tumor response in an immuno-competent setting. This appears to be as a result of immune cell inhibition, suggesting this compound may not be fit for transition into a clinical setting. It may be difficult to find a route of success using this type of inhibitor, with say a checkpoint inhibitor such as PD-L1 or CTLA-4 given that 4T1 cells are not particularly immunogenic. Nonetheless, this type of combinatorial therapy should be a future direction that is taken to see if any success can be derived given that this type of therapy has shown great promise, especially in particular subsets of patients. These experiments with CR-1-31-B treatment should also be repeated with untagged parental 4T1 cells, to rule out any potential confound that the luciferase may have been causing in this particular model. An additional set of important experiments, would be to revisit and continue the preliminary work here presented in regards to the melanoma model. The *in vitro* work presented here showed a strong toward inhibition of B16 melanoma cells when treated with CR-1-31-B. Thus, testing the role of this inhibitor in a relevant mouse model would be paramount. These B16 cells are syngeneic for C57/BL6 mice, and would thus also represent a different mouse background, which could help rule out any differences in response in BALB/c versus C57/BL6 differences in response to eIF4A inhibition.

APPENDIX
Figure 20

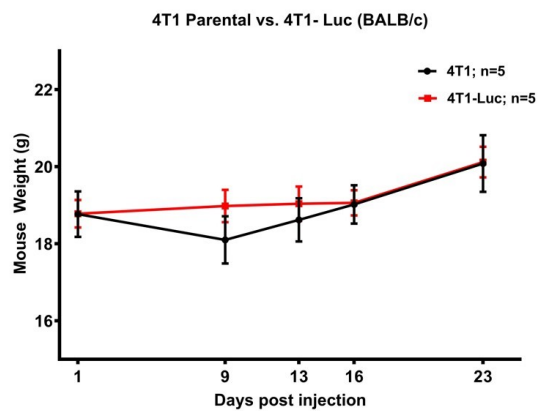
A



B



C



Luciferase Expressing 4T1 Cells have Delayed Tumor Onset and grown in BALB/c mice
(A) Luciferase expressing 4T1 cells have delayed tumor onset in BALB/c mice. For these tumor initiation experiments $P < 0.05$ as calculated using the Mantel-Cox method
(B) Luciferase expressing 4T1 cells produce smaller tumors (assessed via caliper measurement)
(C) Mouse weight in grams
 N=5 per group
 Data are mean \pm SEM (N = 5). * $P < 0.05$.
 2-way ANOVA with Bonferroni Post-Hoc test for caliper measurements of tumor burden.

REFERENCES

1. Dolgin, E., *The most popular genes in the human genome*. Nature, 2017. **551**(7681): p. 427-431.
2. Buttgereit, F. and M.D. Brand, *A hierarchy of ATP-consuming processes in mammalian cells*. Biochem J, 1995. **312** (Pt 1): p. 163-7.
3. Parsyan, A., et al., *mRNA helicases: the tacticians of translational control*. Nat Rev Mol Cell Biol, 2011. **12**(4): p. 235-45.
4. Baker, K.E. and J. Collier, *The many routes to regulating mRNA translation*. Genome Biol, 2006. **7**(12): p. 332.
5. Bin Dhuban, K., et al., *Functional dynamics of Foxp3(+) regulatory T cells in mice and humans*. Immunol Rev, 2014. **259**(1): p. 140-58.
6. Chu, J., et al., *CRISPR-Mediated Drug-Target Validation Reveals Selective Pharmacological Inhibition of the RNA Helicase, eIF4A*. Cell Rep, 2016. **15**(11): p. 2340-7.
7. Hsieh, A.C. and D. Ruggero, *Targeting eukaryotic translation initiation factor 4E (eIF4E) in cancer*. Clin Cancer Res, 2010. **16**(20): p. 4914-20.
8. Moerke, N.J., et al., *Small-molecule inhibition of the interaction between the translation initiation factors eIF4E and eIF4G*. Cell, 2007. **128**(2): p. 257-67.
9. Holcik, M. and N. Sonenberg, *Translational control in stress and apoptosis*. Nat Rev Mol Cell Biol, 2005. **6**(4): p. 318-27.
10. Sonenberg, N., *Cap-binding proteins of eukaryotic messenger RNA: functions in initiation and control of translation*. Prog Nucleic Acid Res Mol Biol, 1988. **35**: p. 173-207.
11. Gingras, A.C., B. Raught, and N. Sonenberg, *eIF4 initiation factors: effectors of mRNA recruitment to ribosomes and regulators of translation*. Annu Rev Biochem, 1999. **68**: p. 913-63.
12. Hiremath, L.S., N.R. Webb, and R.E. Rhoads, *Immunological detection of the messenger RNA cap-binding protein*. J Biol Chem, 1985. **260**(13): p. 7843-9.
13. Duncan, R. and J.W. Hershey, *Identification and quantitation of levels of protein synthesis initiation factors in crude HeLa cell lysates by two-dimensional polyacrylamide gel electrophoresis*. J Biol Chem, 1983. **258**(11): p. 7228-35.
14. Rhoads, R.E., *Cap recognition and the entry of mRNA into the protein synthesis initiation cycle*. Trends Biochem Sci, 1988. **13**(2): p. 52-6.
15. Shatkin, A.J., *Capping of eucaryotic mRNAs*. Cell, 1976. **9**(4 PT 2): p. 645-53.
16. Lazaris-Karatzas, A., K.S. Montine, and N. Sonenberg, *Malignant transformation by a eukaryotic initiation factor subunit that binds to mRNA 5' cap*. Nature, 1990. **345**(6275): p. 544-7.
18. Duncan, R., S.C. Milburn, and J.W. Hershey, *Regulated phosphorylation and low abundance of HeLa cell initiation factor eIF-4F suggest a role in translational control. Heat shock effects on eIF-4F*. J Biol Chem, 1987. **262**(1): p. 380-8.
19. Pestka, S., *The use of inhibitors in studies on protein synthesis*. Methods Enzymol, 1974(0076-6879).
20. Emanuilov, I., et al., *Localization of eukaryotic initiation factor 3 on native small ribosomal subunits*. Proc Natl Acad Sci U S A, 1978. **75**(3): p. 1389-93.

21. Pestova, T.V., et al., *The joining of ribosomal subunits in eukaryotes requires eIF5B*. Nature, 2000. **403**(6767): p. 332-5.
22. Hellen, C.U. and P. Sarnow, *Internal ribosome entry sites in eukaryotic mRNA molecules*. Genes Dev, 2001. **15**(13): p. 1593-612.
23. Kapp, L.D. and J.R. Lorsch, *The molecular mechanics of eukaryotic translation*. Annu Rev Biochem, 2004. **73**: p. 657-704.
24. Rad, E., J.T. Murray, and A.R. Tee, *Oncogenic Signalling through Mechanistic Target of Rapamycin (mTOR): A Driver of Metabolic Transformation and Cancer Progression*. Cancers (Basel), 2018. **10**(1).
25. Hinnebusch, A.G., *The scanning mechanism of eukaryotic translation initiation*. Annu Rev Biochem, 2014. **83**: p. 779-812.
26. Andreev, D.E., et al., *Insights into the mechanisms of eukaryotic translation gained with ribosome profiling*. Nucleic Acids Res, 2017. **45**(2): p. 513-526.
27. Drabkin, H.J. and U.L. RajBhandary, *Initiation of protein synthesis in mammalian cells with codons other than AUG and amino acids other than methionine*. Mol Cell Biol, 1998. **18**(9): p. 5140-7.
28. Kozak, M., *Comparison of initiation of protein synthesis in procaryotes, eucaryotes, and organelles*. Microbiol Rev, 1983. **47**(1): p. 1-45.
29. Kozak, M., *Regulation of translation in eukaryotic systems*. Annu Rev Cell Biol, 1992. **8**: p. 197-225.
30. Kozak, M., *The scanning model for translation: an update*. J Cell Biol, 1989. **108**(2): p. 229-41.
31. Verschoor, A., et al., *Native 3D structure of eukaryotic 80s ribosome: morphological homology with E. coli 70S ribosome*. J Cell Biol, 1996. **133**(3): p. 495-505.
32. Hsieh, A.C., M.L. Truitt, and D. Ruggero, *Oncogenic AKTivation of translation as a therapeutic target*. Br J Cancer, 2011. **105**(3): p. 329-36.
33. Thoreen, C.C., *Many roads from mTOR to eIF4F*. Biochem Soc Trans, 2013. **41**(4): p. 913-6.
34. Wang, X. and C.G. Proud, *The mTOR pathway in the control of protein synthesis*. Physiology (Bethesda), 2006. **21**: p. 362-9.
35. Kanayama, M., et al., *Hyperactive mTOR induces neuroendocrine differentiation in prostate cancer cell with concurrent up-regulation of IRF1*. Prostate, 2017. **77**(15): p. 1489-1498.
36. Morrison Joly, M., et al., *Rictor/mTORC2 Drives Progression and Therapeutic Resistance of HER2-Amplified Breast Cancers*. Cancer Res, 2016. **76**(16): p. 4752-64.
37. Lee, K., et al., *Vital roles of mTOR complex 2 in Notch-driven thymocyte differentiation and leukemia*. J Exp Med, 2012. **209**(4): p. 713-28.
38. Zhou, B.P. and M.C. Hung, *Dysregulation of cellular signaling by HER2/neu in breast cancer*. Semin Oncol, 2003. **30**(5 Suppl 16): p. 38-48.
39. Vivanco, I. and C.L. Sawyers, *The phosphatidylinositol 3-Kinase AKT pathway in human cancer*. Nat Rev Cancer, 2002. **2**(7): p. 489-501.
40. Polunovsky, V.A. and P.B. Bitterman, *The cap-dependent translation apparatus integrates and amplifies cancer pathways*. RNA Biol, 2006. **3**(1): p. 10-7.
41. Menyhart, O., et al., *Guidelines for the selection of functional assays to evaluate the hallmarks of cancer*. Biochim Biophys Acta, 2016. **1866**(2): p. 300-319.
42. Hanahan, D. and R.A. Weinberg, *The hallmarks of cancer*. Cell, 2000. **100**(1): p. 57-70.

43. El-Naggar, A.M. and P.H. Sorensen, *Translational control of aberrant stress responses as a hallmark of cancer*. J Pathol, 2018. **244**(5): p. 650-666.
44. van Zijl, F., G. Krupitza, and W. Mikulits, *Initial steps of metastasis: cell invasion and endothelial transmigration*. Mutat Res, 2011. **728**(1-2): p. 23-34.
45. Sharma, G.N., et al., *Various types and management of breast cancer: an overview*. J Adv Pharm Technol Res, 2010. **1**(2): p. 109-26.
46. Brouckaert, O., et al., *Update on triple-negative breast cancer: prognosis and management strategies*. Int J Womens Health, 2012. **4**: p. 511-20.
47. Blagden, S.P. and A.E. Willis, *The biological and therapeutic relevance of mRNA translation in cancer*. Nat Rev Clin Oncol, 2011. **8**(5): p. 280-91.
48. Parsyan, A., *Translation and its regulation in cancer biology and medicine*. 2016, [Place of publication not identified]: Springer.
49. Hashem, Y. and J. Frank, *The Jigsaw Puzzle of mRNA Translation Initiation in Eukaryotes: A Decade of Structures Unraveling the Mechanics of the Process*. Annu Rev Biophys, 2018.
50. Thach, R.E., *Cap recap: the involvement of eIF-4F in regulating gene expression*. Cell, 1992. **68**(2): p. 177-180.
51. Chu, J. and J. Pelletier, *Therapeutic Opportunities in Eukaryotic Translation*. Cold Spring Harb Perspect Biol, 2018.
52. Carroll, M. and K.L. Borden, *The oncogene eIF4E: using biochemical insights to target cancer*. J Interferon Cytokine Res, 2013. **33**(5): p. 227-38.
53. Pelletier, J., et al., *Targeting the eIF4F translation initiation complex: a critical nexus for cancer development*. Cancer Res, 2015. **75**(2): p. 250-63.
54. Bhat, M., et al., *Targeting the translation machinery in cancer*. Nat Rev Drug Discov, 2015. **14**(4): p. 261-78.
55. Robichaud, N. and N. Sonenberg, *Translational control and the cancer cell response to stress*. Curr Opin Cell Biol, 2017. **45**: p. 102-109.
56. Joyce, C.E., et al., *Differential Regulation of the Melanoma Proteome by eIF4A1 and eIF4E*. Cancer Res, 2017. **77**(3): p. 613-622.
57. Soni, A., et al., *eIF4E knockdown decreases breast cancer cell growth without activating Akt signaling*. Mol Cancer Ther, 2008. **7**(7): p. 1782-8.
58. Robichaud, N., et al., *Translational control in the tumor microenvironment promotes lung metastasis: Phosphorylation of eIF4E in neutrophils*. Proc Natl Acad Sci U S A, 2018. **115**(10): p. E2202-E2209.
59. Wheeler, M.J., P.W. Johnson, and J.P. Blaydes, *The role of MNK proteins and eIF4E phosphorylation in breast cancer cell proliferation and survival*. Cancer Biol Ther, 2010. **10**(7): p. 728-35.
60. Modelska, A., et al., *The malignant phenotype in breast cancer is driven by eIF4A1-mediated changes in the translational landscape*. Cell Death Dis, 2015. **6**: p. e1603.
61. Cencic, R., et al., *Antitumor activity and mechanism of action of the cyclopenta[b]benzofuran, silvestrol*. PLoS One, 2009. **4**(4): p. e5223.
62. Murooka, T.T., R. Rahbar, and E.N. Fish, *CCL5 promotes proliferation of MCF-7 cells through mTOR-dependent mRNA translation*. Biochem Biophys Res Commun, 2009. **387**(2): p. 381-6.
63. Murooka, T.T., et al., *CCL5-mediated T-cell chemotaxis involves the initiation of mRNA translation through mTOR/4E-BP1*. Blood, 2008. **111**(10): p. 4892-901.

64. So, L., et al., *The 4E-BP-eIF4E axis promotes rapamycin-sensitive growth and proliferation in lymphocytes*. *Sci Signal*, 2016. **9**(430): p. ra57.
65. Zou, H., et al., *Synergistic inhibition of colon cancer cell growth with nanoemulsion-loaded paclitaxel and PI3K/mTOR dual inhibitor BEZ235 through apoptosis*. *Int J Nanomedicine*, 2016. **11**: p. 1947-58.
66. Gohr, K., et al., *Inhibition of PI3K/Akt/mTOR overcomes cisplatin resistance in the triple negative breast cancer cell line HCC38*. *BMC Cancer*, 2017. **17**(1): p. 711.
67. Chapman, N.M. and H. Chi, *mTOR signaling, Tregs and immune modulation*. *Immunotherapy*, 2014. **6**(12): p. 1295-311.
68. Kim, K.W., et al., *The effect of mammalian target of rapamycin inhibition on T helper type 17 and regulatory T cell differentiation in vitro and in vivo in kidney transplant recipients*. *Immunology*, 2015. **144**(1): p. 68-78.
69. Battaglia, M., et al., *Rapamycin promotes expansion of functional CD4⁺CD25⁺FOXP3⁺ regulatory T cells of both healthy subjects and type 1 diabetic patients*. *J Immunol*, 2006. **177**(12): p. 8338-47.
70. Chapman, N.M. and H. Chi, *mTOR Links Environmental Signals to T Cell Fate Decisions*. *Front Immunol*, 2014. **5**: p. 686.
71. Bilate, A.M. and J.J. Lafaille, *Induced CD4⁺Foxp3⁺ regulatory T cells in immune tolerance*. *Annu Rev Immunol*, 2012. **30**: p. 733-58.
72. Bjur, E., et al., *Distinct translational control in CD4⁺ T cell subsets*. *PLoS Genet*, 2013. **9**(5): p. e1003494.
73. Piccirillo, C.A., et al., *Translational control of immune responses: from transcripts to translatoemes*. *Nat Immunol*, 2014. **15**(6): p. 503-11.
74. Svitkin, Y.V., et al., *The requirement for eukaryotic initiation factor 4A (eIF4A) in translation is in direct proportion to the degree of mRNA 5' secondary structure*. *RNA*, 2001. **7**(3): p. 382-94.
75. Pelletier, J. and N. Sonenberg, *Insertion mutagenesis to increase secondary structure within the 5' noncoding region of a eukaryotic mRNA reduces translational efficiency*. *Cell*, 1985. **40**(3): p. 515-26.
76. Kozak, M., *Influences of mRNA secondary structure on initiation by eukaryotic ribosomes*. *Proc Natl Acad Sci U S A*, 1986. **83**(9): p. 2850-4.
77. Mignone, F., et al., *Untranslated regions of mRNAs*. *Genome Biol*, 2002. **3**(3): p. REVIEWS0004.
78. Koromilas, A.E., A. Lazaris-Karatzas, and N. Sonenberg, *mRNAs containing extensive secondary structure in their 5' non-coding region translate efficiently in cells overexpressing initiation factor eIF-4E*. *EMBO J*, 1992. **11**(11): p. 4153-8.
79. Ruggero, D. and N. Sonenberg, *The Akt of translational control*. *Oncogene*, 2005. **24**(50): p. 7426-34.
80. Birch, J., et al., *The initiator methionine tRNA drives cell migration and invasion leading to increased metastatic potential in melanoma*. *Biol Open*, 2016. **5**(10): p. 1371-1379.
81. Feoktistova, K., et al., *Human eIF4E promotes mRNA restructuring by stimulating eIF4A helicase activity*. *Proc Natl Acad Sci U S A*, 2013. **110**(33): p. 13339-44.
82. Barrett, L.W., S. Fletcher, and S.D. Wilton, *Regulation of eukaryotic gene expression by the untranslated gene regions and other non-coding elements*. *Cell Mol Life Sci*, 2012. **69**(21): p. 3613-34.

83. Sen, N.D., et al., *eIF4B stimulates translation of long mRNAs with structured 5' UTRs and low closed-loop potential but weak dependence on eIF4G*. Proc Natl Acad Sci U S A, 2016. **113**(38): p. 10464-72.
84. Rozen, F., et al., *Bidirectional RNA helicase activity of eucaryotic translation initiation factors 4A and 4F*. Mol Cell Biol, 1990. **10**(3): p. 1134-44.
85. Wolfe, A.L., et al., *RNA G-quadruplexes cause eIF4A-dependent oncogene translation in cancer*. Nature, 2014. **513**(7516): p. 65-70.
86. Vaysse, C., et al., *Key contribution of eIF4H-mediated translational control in tumor promotion*. Oncotarget, 2015. **6**(37): p. 39924-40.
87. Low, W.K., et al., *Inhibition of eukaryotic translation initiation by the marine natural product pateamine A*. Mol Cell, 2005. **20**(5): p. 709-22.
88. Popa, A., et al., *Pateamine A-sensitive ribosome profiling reveals the scope of translation in mouse embryonic stem cells*. BMC Genomics, 2016. **17**: p. 52.
89. Li-Weber, M., *Molecular mechanisms and anti-cancer aspects of the medicinal phytochemicals rocaglamides (=flavaglines)*. Int J Cancer, 2015. **137**(8): p. 1791-9.
90. Becker, M.S., et al., *The anticancer phytochemical rocaglamide inhibits Rho GTPase activity and cancer cell migration*. Oncotarget, 2016. **7**(32): p. 51908-51921.
91. Rubio, C.A., et al., *Transcriptome-wide characterization of the eIF4A signature highlights plasticity in translation regulation*. Genome Biol, 2014. **15**(10): p. 476.
92. Duffy, A.G., et al., *Modulation of tumor eIF4E by antisense inhibition: A phase I/II translational clinical trial of ISIS 183750-an antisense oligonucleotide against eIF4E-in combination with irinotecan in solid tumors and irinotecan-refractory colorectal cancer*. Int J Cancer, 2016. **139**(7): p. 1648-57.
93. Gandin, V., et al., *nanoCAGE reveals 5' UTR features that define specific modes of translation of functionally related MTOR-sensitive mRNAs*. Genome Res, 2016. **26**(5): p. 636-48.
94. Chu, J. and J. Pelletier, *Targeting the eIF4A RNA helicase as an anti-neoplastic approach*. Biochim Biophys Acta, 2015. **1849**(7): p. 781-91.
95. Baklaushev, V.P., et al., *Luciferase Expression Allows Bioluminescence Imaging But Imposes Limitations on the Orthotopic Mouse (4T1) Model of Breast Cancer*. Sci Rep, 2017. **7**(1): p. 7715.
96. Tao, K., et al., *Imagable 4T1 model for the study of late stage breast cancer*. BMC Cancer, 2008. **8**: p. 228.
97. Tang, D., et al., *HMGB1 release and redox regulates autophagy and apoptosis in cancer cells*. Oncogene, 2010. **29**(38): p. 5299-310.
98. Stone, M.K., et al., *p38 mitogen-activated protein kinase mediates lipopolysaccharide and tumor necrosis factor alpha induction of shiga toxin 2 sensitivity in human umbilical vein endothelial cells*. Infect Immun, 2008. **76**(3): p. 1115-21.
99. Samokhvalov, V., et al., *PPARdelta signaling mediates the cytotoxicity of DHA in H9c2 cells*. Toxicol Lett, 2015. **232**(1): p. 10-20.
100. Ioannou, M.S., et al., *DENND2B activates Rab13 at the leading edge of migrating cells and promotes metastatic behavior*. J Cell Biol, 2015. **208**(5): p. 629-48.
101. Robichaud, N., et al., *Phosphorylation of eIF4E promotes EMT and metastasis via translational control of SNAIL and MMP-3*. Oncogene, 2015. **34**(16): p. 2032-42.
102. Sommers, C.L., et al., *Differentiation state and invasiveness of human breast cancer cell lines*. Breast Cancer Res Treat, 1994. **31**(2-3): p. 325-35.

103. Chen, H.C., *Boyden chamber assay*. Methods Mol Biol., 2005(1064-3745 (Print)).
104. Feoktistova, M., P. Geserick, and M. Leverkus, *Crystal Violet Assay for Determining Viability of Cultured Cells*. Cold Spring Harb Protoc, 2016. **2016**(4): p. pdb prot087379.
105. Zhou, X., et al., *Overexpression of MPC1 inhibits the proliferation, migration, invasion, and stem cell-like properties of gastric cancer cells*. Onco Targets Ther, 2017. **10**: p. 5151-5163.
106. Chen, W., et al., *Human astrocytes secrete IL-6 to promote glioma migration and invasion through upregulation of cytomembrane MMP14*. Oncotarget, 2016. **7**(38): p. 62425-62438.
107. Dai, M., et al., *A novel function for p21Cip1 and acetyltransferase p/CAF as critical transcriptional regulators of TGFbeta-mediated breast cancer cell migration and invasion*. Breast Cancer Res, 2012. **14**(5): p. R127.
108. Harma, V., et al., *Quantification of dynamic morphological drug responses in 3D organotypic cell cultures by automated image analysis*. PLoS One, 2014. **9**(5): p. e96426.
109. Khoutorsky, A., et al., *Translational control of nociception via 4E-binding protein 1*. Elife, 2015. **4**.
110. Malka-Mahieu, H., et al., *Synergistic effects of eIF4A and MEK inhibitors on proliferation of NRAS-mutant melanoma cell lines*. Cell Cycle, 2016. **15**(18): p. 2405-9.
111. Bordeleau, M.E., et al., *Therapeutic suppression of translation initiation modulates chemosensitivity in a mouse lymphoma model*. J Clin Invest, 2008. **118**(7): p. 2651-60.
112. Kogure, T., et al., *Therapeutic potential of the translation inhibitor silvestrol in hepatocellular cancer*. PLoS One, 2013. **8**(9): p. e76136.
113. Daker, M., et al., *Inhibition of nasopharyngeal carcinoma cell proliferation and synergism of cisplatin with silvestrol and episilvestrol isolated from Aglaia stellatopilosa*. Exp Ther Med, 2016. **11**(6): p. 2117-2126.
114. Lopez-Saez, J.F., et al., *Cell proliferation and cancer*. Histol Histopathol, 1998. **13**(4): p. 1197-214.
115. Feitelson, M.A., et al., *Sustained proliferation in cancer: Mechanisms and novel therapeutic targets*. Semin Cancer Biol, 2015. **35 Suppl**: p. S25-S54.
116. Kawazu, M., et al., *Transforming mutations of RAC guanosine triphosphatases in human cancers*. Proc Natl Acad Sci U S A, 2013. **110**(8): p. 3029-34.
117. Schnelzer, A., et al., *Rac1 in human breast cancer: overexpression, mutation analysis, and characterization of a new isoform, Rac1b*. Oncogene, 2000. **19**(26): p. 3013-20.
118. Sosa, M.S., et al., *Identification of the Rac-GEF P-Rex1 as an essential mediator of ErbB signaling in breast cancer*. Mol Cell, 2010. **40**(6): p. 877-92.
119. Chaffer, C.L. and R.A. Weinberg, *A perspective on cancer cell metastasis*. Science, 2011. **331**(6024): p. 1559-64.
120. Wolf, K., et al., *Multi-step pericellular proteolysis controls the transition from individual to collective cancer cell invasion*. Nat Cell Biol, 2007. **9**(8): p. 893-904.
121. Croft, D.R. and M.F. Olson, *Regulating the conversion between rounded and elongated modes of cancer cell movement*. Cancer Cell, 2008. **14**(5): p. 349-51.
122. Kabla, A.J., *Collective cell migration: leadership, invasion and segregation*. J R Soc Interface, 2012. **9**(77): p. 3268-78.
123. Zengel, P., et al., *mu-Slide Chemotaxis: a new chamber for long-term chemotaxis studies*. BMC Cell Biol, 2011. **12**: p. 21.

124. Kramer, N., et al., *In vitro cell migration and invasion assays*. *Mutat Res*, 2013. **752**(1): p. 10-24.
125. Franken, N.A., et al., *Clonogenic assay of cells in vitro*. *Nat Protoc*, 2006. **1**(5): p. 2315-9.
126. Tsukumo, Y., et al., *Translation control during prolonged mTORC1 inhibition mediated by 4E-BP3*. *Nat Commun*, 2016. **7**: p. 11776.
127. Schmidt, E.K., et al., *SUnSET, a nonradioactive method to monitor protein synthesis*. *Nat Methods*, 2009. **6**(4): p. 275-7.
128. Watanabe, Y., et al., *The analysis of the functions of human B and T cells in humanized NOD/shi-scid/gammac(null) (NOG) mice (hu-HSC NOG mice)*. *Int Immunol*, 2009. **21**(7): p. 843-58.
129. Tang, H., et al., *Facilitating T Cell Infiltration in Tumor Microenvironment Overcomes Resistance to PD-L1 Blockade*. *Cancer Cell*, 2016. **29**(3): p. 285-296.
130. Rodrigo, C.M., et al., *Synthesis of rocaglamide hydroxamates and related compounds as eukaryotic translation inhibitors: synthetic and biological studies*. *J Med Chem*, 2012. **55**(1): p. 558-62.
131. Boussemart, L., et al., *eIF4F is a nexus of resistance to anti-BRAF and anti-MEK cancer therapies*. *Nature*, 2014. **513**(7516): p. 105-9.
132. Mamane, Y., et al., *Epigenetic activation of a subset of mRNAs by eIF4E explains its effects on cell proliferation*. *PLoS One*, 2007. **2**(2): p. e242.
133. Ilic, N., et al., *PI3K-targeted therapy can be evaded by gene amplification along the MYC-eukaryotic translation initiation factor 4E (eIF4E) axis*. *Proc Natl Acad Sci U S A*, 2011. **108**(37): p. E699-708.
134. Wiegner, A., et al., *Targeting Translation Initiation Bypasses Signaling Crosstalk Mechanisms That Maintain High MYC Levels in Colorectal Cancer*. *Cancer Discov*, 2015. **5**(7): p. 768-781.
135. Iwasaki, S., S.N. Floor, and N.T. Ingolia, *Rocaglates convert DEAD-box protein eIF4A into a sequence-selective translational repressor*. *Nature*, 2016. **534**(7608): p. 558-61.
136. Byers, H.R., et al., *Cell migration and actin organization in cultured human primary, recurrent cutaneous and metastatic melanoma. Time-lapse and image analysis*. *Am J Pathol*, 1991. **139**(2): p. 423-35.
137. Liu, J., et al., *Exo70 stimulates the Arp2/3 complex for lamellipodia formation and directional cell migration*. *Curr Biol*, 2012. **22**(16): p. 1510-5.

